

Effective chiral response of anisotropic multilayered metamaterials

Konstantin Baranov,^{1,*} Dmitry Vagin,^{1,*} and Maxim A. Gorlach^{1,†}

¹*School of Physics and Engineering, ITMO University, Saint Petersburg 197101, Russia*

We consider a multilayered metamaterial composed of anisotropic layers with in-plane anisotropy axes periodically rotated with respect to each other. Due to the breaking of inversion symmetry, the structure develops an effective chirality. We derive the effective chirality tensor of the metamaterial describing both normal and oblique incidence scenarios. We also identify the arrangement of the layers maximizing chiral response for the fixed lattice period, wavelength and anisotropy of the layers.

I. INTRODUCTION

One of the most salient features of metamaterials is the emergence of effective properties beyond those of their constituent elements. While elementary building blocks of the structure are ordinary metals or dielectrics, their collective response to the electromagnetic excitation can be quite nontrivial. Besides celebrated negative effective permittivity and permeability [1–3], emergent properties include various forms of electromagnetic non-reciprocity [4, 5], nonlocality [6, 7] and even effective axion fields [8, 9].

One of such useful properties is chirality which is broadly defined as impossibility to superimpose object with its mirror image. Specifically, we focus on *electromagnetic chirality* that couples electric and magnetic responses of the medium, ensures different interaction of the medium with left- and right-hand circularly polarized waves [10–12] and originates due to the breaking of inversion symmetry. While different measures of chirality are discussed in the literature [13–15], here we introduce it as a tensor $\hat{\kappa}$ arising in the bulk material equations [16]

$$\begin{cases} \mathbf{D} = \hat{\varepsilon}\mathbf{E} + i\hat{\kappa}\mathbf{H}, \\ \mathbf{B} = -i\hat{\kappa}^T\mathbf{E} + \hat{\mu}\mathbf{H}, \end{cases} \quad (1)$$

where $\hat{\varepsilon}$ and $\hat{\mu}$ are the conventional permittivity and permeability.

Chirality is ubiquitous in organic materials, where it stems from the non-centrosymmetric nature of the constituent molecules and can hardly be tuned. At the classical level, this physics is captured by the Born-Kuhn model [17]; quantum-mechanical description is also available [18].

At the same time, chirality can also be configurational arising due to the proper non-symmetric arrangement of centrosymmetric elements [19, 20]. This is the case for cholesteric liquid crystals utilized for LC displays technology [21, 22]. More recently, helical homostructures have been realized by stacking biaxial van der Waals crystals exhibiting large permittivity up to 10 along with strong

anisotropy [23]. These experimental advances open a route to tailor chiral response of optical nanostructures.

However, the detailed theoretical understanding of emergent chirality is currently lacking. As previous studies focused on the normal incidence scenario and extracted only single component of chirality [19, 23], full tensor $\hat{\kappa}$ remained unknown. Furthermore, emergent chirality depends on the specific way how anisotropic layers are rotated with respect to each other. While uniform rotation from layer to layer is the most straightforward option, other arrangements are also possible and could potentially bring richer phenomena.

In this Article, we aim to fill this gap and develop an effective medium description of a metamaterial composed of anisotropic layers with in-plane anisotropy axes rotated with respect to each other. Building on homogenization theory [24, 25], we retrieve the full set of the effective material parameters capturing normal and oblique incidence geometry. The obtained results are general and encompass the entire family of structures with arbitrary periodic law of anisotropy axis rotation. In turn, this allows us to maximize the effective chirality depending on the layer arrangement for the fixed period, wavelength and layer permittivities.

The rest of the Article is organized as follows. In Sec. II we examine the symmetry constraints on the structure of chirality tensor. We outline our approach for the normal incidence scenario in Sec. III and compare the key predictions with the rigorous transfer matrix method in Sec. IV. Having validated the analytical results, in Sec. V we identify the arrangement of the layers favoring maximal chiral response. Eventually in Sec. VI we reconstruct full chirality tensor featuring somewhat counter-intuitive structure. Finally, we conclude by Sec. VII summarizing our results and outlining future perspectives.

II. SYMMETRY ANALYSIS

We examine a multilayered metamaterial formed by stacking anisotropic layers with the principal components of permittivity tensor ε_1 , ε_2 and ε_3 . The layers are periodically rotated with respect to each other such that one of their anisotropy axes remains in *Oxy* plane forming angle $\alpha(z)$ with the *x* axis, see Fig. 1(a).

If the period of the lattice *a* is much smaller than the

* These authors have contributed equally to this work

† m.gorlach@metalab.ifmo.ru

wavelength λ , the whole structure behaves as an effective medium and its material equations to some approximation can be presented in the form Eq. (1). The tensors $\hat{\varepsilon}$, $\hat{\mu}$ and $\hat{\kappa}$ entering those equations are constrained by the symmetries of the meta-structure, which we analyze below.

We start from the simplest option when the layers are very thin compared to the lattice period and the anisotropy axis rotates uniformly from layer to layer:

$$\alpha(z) = \frac{\pi z}{a}, \quad (2)$$

which we further call spiral symmetry. In such case, the symmetry group of the structure includes $C_2^{(x)}$ rotation with respect to the x axis and the combination of arbitrary rotation $C_\alpha^{(z)}$ relative to the z axis followed by the proportional shift [Fig. 1(b)]. Since translations do not affect bulk material parameters, chirality tensor has to satisfy

$$\hat{\kappa} = \pm \hat{R}(g) \hat{\kappa} \hat{R}^{-1}(g), \quad (3)$$

where g is a symmetry element which is either $C_2^{(x)}$ or $C_\alpha^{(z)}$ with arbitrary angle α . \hat{R} is a matrix of the respective transformation and the sign in Eq. (3) depends on the sign of the determinant $\det \hat{R}$, e.g. $+$ for proper rotations, $-$ for reflections. Straightforward calculation yields that in the case of spiral symmetry chirality tensor is necessarily diagonal:

$$\hat{\kappa} = \text{diag}(\kappa_{11}, \kappa_{11}, \kappa_{33}), \quad (4)$$

but not necessarily isotropic, i.e. $\kappa_{11} \neq \kappa_{33}$. In fact, κ_{33} component is not manifested in normal incidence geometry and can only be probed at oblique incidence. Note that in practice the combination of symmetries $C_2^{(x)}$ and $C_n^{(z)}$ with $n \geq 3$ suffice to ensure the diagonal structure of chirality tensor, Eq. (4).

In the same spirit, we examine more general scenario with the arbitrary law $\alpha(z)$ of anisotropy axis rotation with the only requirement $\alpha(0) = \alpha(a) = 0$ [Fig. 1(c)]. This lowers the symmetry of the structure down to $C_2^{(z)}$ leaving a single symmetry element and resulting in a more complicated chirality tensor

$$\hat{\kappa}^{(\text{arb})} = \begin{pmatrix} \kappa_{11} & \kappa_{12} & 0 \\ \kappa_{21} & \kappa_{22} & 0 \\ 0 & 0 & \kappa_{33} \end{pmatrix}. \quad (5)$$

Besides anisotropic chirality, the system develops two more responses: pseudochirality captured by the symmetric zero-trace part of the matrix Eq. (5) and omega-type response characterized by the antisymmetric part of Eq. (5). The distinction between the two responses also depends on symmetry.

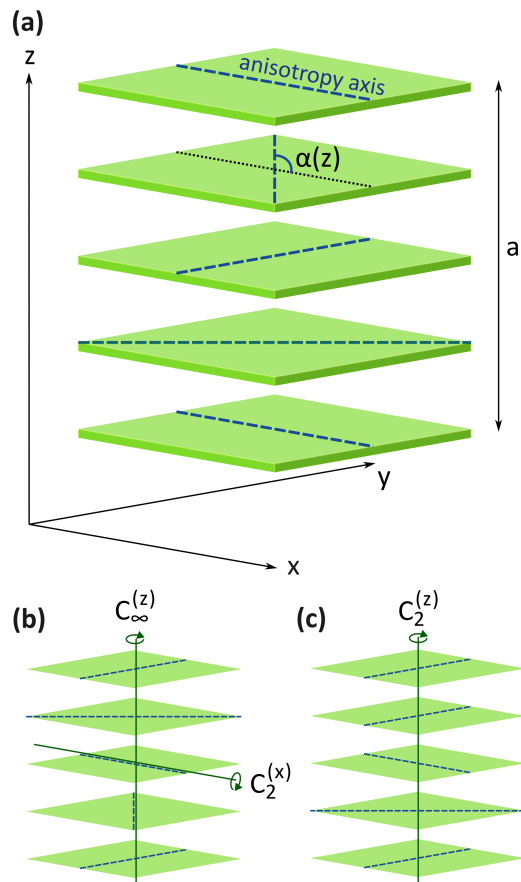


FIG. 1. (a) A sketch of the multilayered structure composed of anisotropic layers rotated relative to each other. (b) Point symmetry axes in case of spiral symmetry. (c) Point symmetry axis for the arbitrary rotation of the layers $\alpha(z)$.

III. DERIVATION OF THE EFFECTIVE MATERIAL PARAMETERS: NORMAL INCIDENCE SCENARIO

In our theoretical analysis, we assume that the first anisotropic layer is located at $z = 0$ possessing the permittivity tensor

$$\hat{\varepsilon}_{01} = \begin{pmatrix} \varepsilon_1 & 0 & 0 \\ 0 & \varepsilon_2 & 0 \\ 0 & 0 & \varepsilon_3 \end{pmatrix}. \quad (6)$$

Other layers with identical properties are rotated by different angles α in Oxy plane. Hence, the permittivity of the layer with the coordinate z is given by

$$\begin{aligned} \hat{\varepsilon}(z) &= \hat{R}(\alpha) \hat{\varepsilon}_{01} \hat{R}^{-1}(\alpha) \\ &= \begin{pmatrix} \bar{\varepsilon} & 0 & 0 \\ 0 & \bar{\varepsilon} & 0 \\ 0 & 0 & \varepsilon_3 \end{pmatrix} + \Delta\varepsilon \begin{pmatrix} -\cos(2\alpha) & -\sin(2\alpha) & 0 \\ -\sin(2\alpha) & \cos(2\alpha) & 0 \\ 0 & 0 & 0 \end{pmatrix}, \quad (7) \end{aligned}$$

where \hat{R} matrix describes counterclockwise rotation with respect to z axis

$$\hat{R}(\alpha) = \begin{pmatrix} \cos \alpha & -\sin \alpha & 0 \\ \sin \alpha & \cos \alpha & 0 \\ 0 & 0 & 1 \end{pmatrix}, \quad (8)$$

$\bar{\varepsilon} = (\varepsilon_1 + \varepsilon_2)/2$ is the average permittivity, $\Delta\varepsilon = (\varepsilon_2 - \varepsilon_1)/2$ is the half-difference between the principal permittivity components and $b = 2\pi/a$ is the reciprocal lattice period.

In the case of monochromatic fields and monochromatic external sources \mathbf{j} Maxwell's equations yield

$$\Delta \mathbf{E} - \nabla(\text{div } \mathbf{E}) + q^2 \mathbf{D} = -\frac{4\pi i q}{c} \mathbf{j}, \quad (9)$$

where $q = \omega/c$, ω is the frequency of the wave, c is the speed of light and CGS system of units is employed.

Periodicity of the system allows to expand the electric field in the form

$$\mathbf{E}(\mathbf{r}) = \sum_n \mathbf{E}_n \exp[i\mathbf{k}_\perp \cdot \mathbf{r} + i(k_z + nb)z], \quad (10)$$

where \mathbf{E}_n are the Floquet harmonics of electric field, \mathbf{k} is the wave vector with in-plane component \mathbf{k}_\perp and the similar expansion is valid for the electric displacement \mathbf{D} .

Deriving the effective medium description, we focus on the behavior of the *averaged* fields represented by the zeroth order Floquet harmonic of the expansion Eq. (10). Assuming that the external current density \mathbf{j} has only zeroth order Floquet harmonic \mathbf{j}_0 , we aim to compute higher-order Floquet harmonics in terms of the averaged fields and recover the link between \mathbf{D}_0 and \mathbf{E}_0 , which defines the effective material parameters of interest. In turn, the presence of external sources \mathbf{j} allows to distinguish frequency and spatial dispersion as \mathbf{k} and ω become independent.

To illustrate the above strategy, we consider first the scenario when the wave vector is orthogonal to the layers, $\mathbf{k} = (0, 0, k_z)^\top$, while electric field lies in the Oxy plane: $\mathbf{E} = (E_x, E_y, 0)^\top$. As the electric field is orthogonal to \mathbf{k} and $\mathbf{k} + nb \mathbf{e}_z$, the problem simplifies, $\nabla(\text{div } \mathbf{E})$ drops out from Eq. (9) and we immediately recover the connection between higher-order Floquet harmonics of electric field and displacement:

$$\mathbf{E}_n = \frac{q^2}{(k_z + nb)^2} \mathbf{D}_n \approx \frac{q^2}{n^2 b^2} \left(1 - \frac{2k_z}{nb}\right) \mathbf{D}_n + O(\xi^4), \quad (11)$$

where $\xi = q/b = a/\lambda$ is a small parameter and $n \neq 0$.

On the other hand, electric field and electric displacement at a given point are related to each other via the usual constitutive relation $\mathbf{D}(z) = \hat{\varepsilon}(z) \mathbf{E}(z)$. Expanding the permittivity in the Fourier series $\hat{\varepsilon}(z) = \sum_n \hat{\varepsilon}_n e^{inbz}$ and using the Floquet expansion of the fields, Eq. (10), we recover

$$\mathbf{D}_n = \sum_{n'} \hat{\varepsilon}_{n-n'} \mathbf{E}_{n'} = \hat{\varepsilon}_n \mathbf{E}_0 + O(\xi^2). \quad (12)$$

Combining Eqs. (11) and (12), we deduce the averaged displacement in the form

$$\begin{aligned} \mathbf{D}_0 &= \sum_n \hat{\varepsilon}_{-n} \mathbf{E}_n = \hat{\varepsilon}_0 \mathbf{E}_0 + \sum_{n \neq 0} \hat{\varepsilon}_{-n} \mathbf{E}_n \approx \\ &\approx \hat{\varepsilon}_0 \mathbf{E}_0 + \frac{q^2}{b^2} \sum_{n \neq 0} \frac{\hat{\varepsilon}_{-n} \hat{\varepsilon}_n}{n^2} \mathbf{E}_0 - \frac{2k_z q^2}{b^3} \sum_{n \neq 0} \frac{\hat{\varepsilon}_{-n} \hat{\varepsilon}_n}{n^3} \mathbf{E}_0 = \\ &= \left[\hat{\varepsilon}_0 + \frac{q^2}{b^2} \sum_{n=1}^{\infty} \frac{\{\hat{\varepsilon}_{-n}, \hat{\varepsilon}_n\}}{n^2} \right] \mathbf{E}_0 - \frac{2k_z q^2}{b^3} \sum_{n=1}^{\infty} \frac{[\hat{\varepsilon}_{-n}, \hat{\varepsilon}_n]}{n^3} \mathbf{E}_0, \end{aligned} \quad (13)$$

where the terms proportional to ξ^4 or higher powers of small parameter ξ are neglected.

Such connection between the averaged fields is a typical example of *spatial dispersion*, when the electric displacement depends not only on the field at the same point, but also on its spatial derivatives (see the term $\propto k_z$). However, the first derivative of \mathbf{E} yields magnetic field \mathbf{H} and therefore such corrections are equivalent to bianisotropy [16] with the material equations Eq. (1). The connection between the nonlocal permittivity tensor $\hat{\varepsilon}(\omega, \mathbf{k})$ and local effective material parameters $\hat{\varepsilon}$ and $\hat{\kappa}$ reads [24]:

$$\hat{\varepsilon}(\omega, \mathbf{k}) = [\hat{\varepsilon} - \hat{\kappa} \hat{\kappa}^\top] + \frac{i}{q} [\hat{\kappa} \mathbf{k}^\times + \mathbf{k}^\times \hat{\kappa}^\top], \quad (14)$$

where $\mathbf{k}_{il} = e_{ijl} k_j$ and e_{ijl} is a fully antisymmetric tensor with $e_{123} = 1$.

For the general structure of chirality tensor Eq. (5) and normal incidence geometry, spatial dispersion correction in Eq. (14) takes a simple form

$$\delta \hat{\varepsilon}(\omega, \mathbf{k}) = 2i\kappa_{\text{eff}} k_z / q \mathbf{e}_z^\times, \quad (15)$$

where $\kappa_{\text{eff}} = (\kappa_{11} + \kappa_{22})/2$. To proceed further, we evaluate $\hat{\varepsilon}_n$ Fourier components with $n \neq 0$ explicitly from Eq. (7):

$$\hat{\varepsilon}_n \equiv \frac{1}{a} \int_0^a \hat{\varepsilon}(z) e^{-inbz} dz = -\Delta\varepsilon (\sigma_z C_n + \sigma_x S_n), \quad (16)$$

where we consider xy subspace, σ_x and σ_z denote Pauli matrices and the dimensionless coefficients C_n and S_n are given by

$$C_n = \frac{1}{a} \int_0^a e^{-inbz} \cos 2\alpha(z) dz, \quad (17)$$

$$S_n = \frac{1}{a} \int_0^a e^{-inbz} \sin 2\alpha(z) dz \quad (18)$$

and depend on the specific way how the anisotropy axis is rotated from layer to layer.

Straightforward calculation and the comparison of Eqs. (13), (15) yield the general expression for effective chirality

$$\kappa_{\text{eff}} = -\frac{4\Delta\varepsilon^2 q^3}{b^3} \sum_{n=1}^{\infty} \frac{\text{Im}(C_n S_n^*)}{n^3}, \quad (19)$$

while xx and yy components of effective permittivity read

$$\varepsilon_{\text{eff}} = \bar{\varepsilon} + \frac{2q^2\Delta\varepsilon^2}{b^2} \sum_{n=1}^{\infty} \frac{|C_n|^2 + |S_n|^2}{n^2}. \quad (20)$$

Equations (19),(20) define the effective material parameters of a multilayer for the arbitrary law of anisotropy axis rotation. Interestingly, the correction to the effective permittivity appears already in the second order in $\xi = q/b$, while chirality arises only in the third order vanishing in the subwavelength limit $\xi \ll 1$.

It is instructive to examine the case of spiral medium with a specific law of anisotropy axis rotation, Eq. (2). In this case, for $n \geq 1$ $C_n = 1/2\delta_{n1}$ and $S_n = -i/2\delta_{n1}$ and thus

$$\varepsilon_{\text{eff}} = \bar{\varepsilon} + \Delta\varepsilon^2 \frac{q^2}{b^2}, \quad (21)$$

$$\kappa_{\text{eff}} = -\Delta\varepsilon^2 \frac{q^3}{b^3}. \quad (22)$$

Note that the latter equations were obtained previously [19, 23] without using homogenization theory but examining the eigenmodes of a spiral medium instead (Supplementary Materials, Sec. I). Indeed, electromagnetic chirality is imprinted in the structure of the eigenmodes which have circular polarizations and different refractive indices

$$n_{\pm} = \sqrt{\varepsilon\mu} \pm \kappa, \quad (23)$$

which allows to probe chirality via eigenmode simulations.

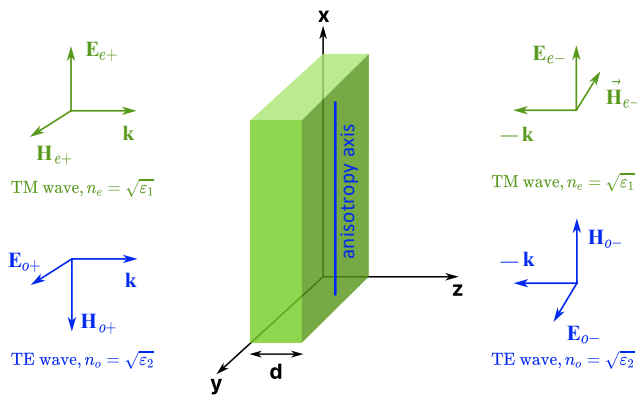


FIG. 2. Reflection and transmission of waves in anisotropic dielectric slab and construction of the transfer matrix.

It should be stressed that the solution Eqs. (19), (20) presented here is more general and allows to compute chiral response in other physically relevant situations – for instance, when the unit cell of the lattice contains few anisotropic layers and the rotation of anisotropy axis from layer to layer is not continuous but rather stepwise (see Supplementary Materials, Sec. II).

IV. VALIDATION OF THE EFFECTIVE MEDIUM DESCRIPTION

To test the validity of the effective medium description, we simulate multilayered metamaterial using rigorous transfer matrix method. We introduce the vector of the fields $\mathbf{v} = (E_x, E_y, H_x, H_y)^T$ and define the transfer matrix as

$$\mathbf{v}(d) = \hat{M}(d) \mathbf{v}(0). \quad (24)$$

Then, given the eigenmodes of anisotropic dielectric [Fig. 2], the transfer matrix $\hat{M}(d)$ for the homogeneous slab with x -oriented anisotropy axis reads

$$\begin{pmatrix} \cos(qn_e d) & 0 & 0 & \frac{i}{n_e} \sin(qn_e d) \\ 0 & \cos(qn_o d) & -\frac{i}{n_o} \sin(qn_o d) & 0 \\ 0 & -in_o \sin(qn_o d) & \cos(qn_o d) & 0 \\ in_e \sin(qn_e d) & 0 & 0 & \cos(qn_e d) \end{pmatrix}.$$

If the layer is rotated, its transfer matrix is computed as

$$\hat{M}_m = \hat{T}(\alpha_m) \hat{M}_0 \hat{T}^{-1}(\alpha_m),$$

with

$$\hat{T}(\alpha) = \begin{pmatrix} R_2(\alpha) & 0_2 \\ 0_2 & R_2(\alpha) \end{pmatrix},$$

where $R_2(\alpha)$ is the xy block of the rotation matrix Eq. (8) and 0_2 is 2×2 zero matrix. The transfer matrix for the lattice period is recovered by multiplying the matrices of all constituent layers

$$\hat{M}_{\text{period}} = \hat{M}_N \cdot \hat{M}_{N-1} \cdot \dots \cdot \hat{M}_2 \cdot \hat{M}_1 \cdot \hat{M}_0. \quad (25)$$

The eigenmodes of the periodic structure are found from the equation

$$\left[\hat{M}_{\text{period}} - e^{ik_z a} \right] \mathbf{v}(0) = 0, \quad (26)$$

where the eigenvalues k_z are related to the refractive indices of the eigenmodes, while the respective eigenvectors \mathbf{v} define their polarization at the point $z = 0$.

We solve Eq. (26) for experimentally relevant parameters [23] at normal incidence ($k_z = nq$). Assuming that the lattice period is formed by $N = 15$ anisotropic layers with a uniform rotation of anisotropy axis from layer to layer, in Fig. 3(a) we plot the difference of the refractive indices of the two forward-propagating eigenmodes which

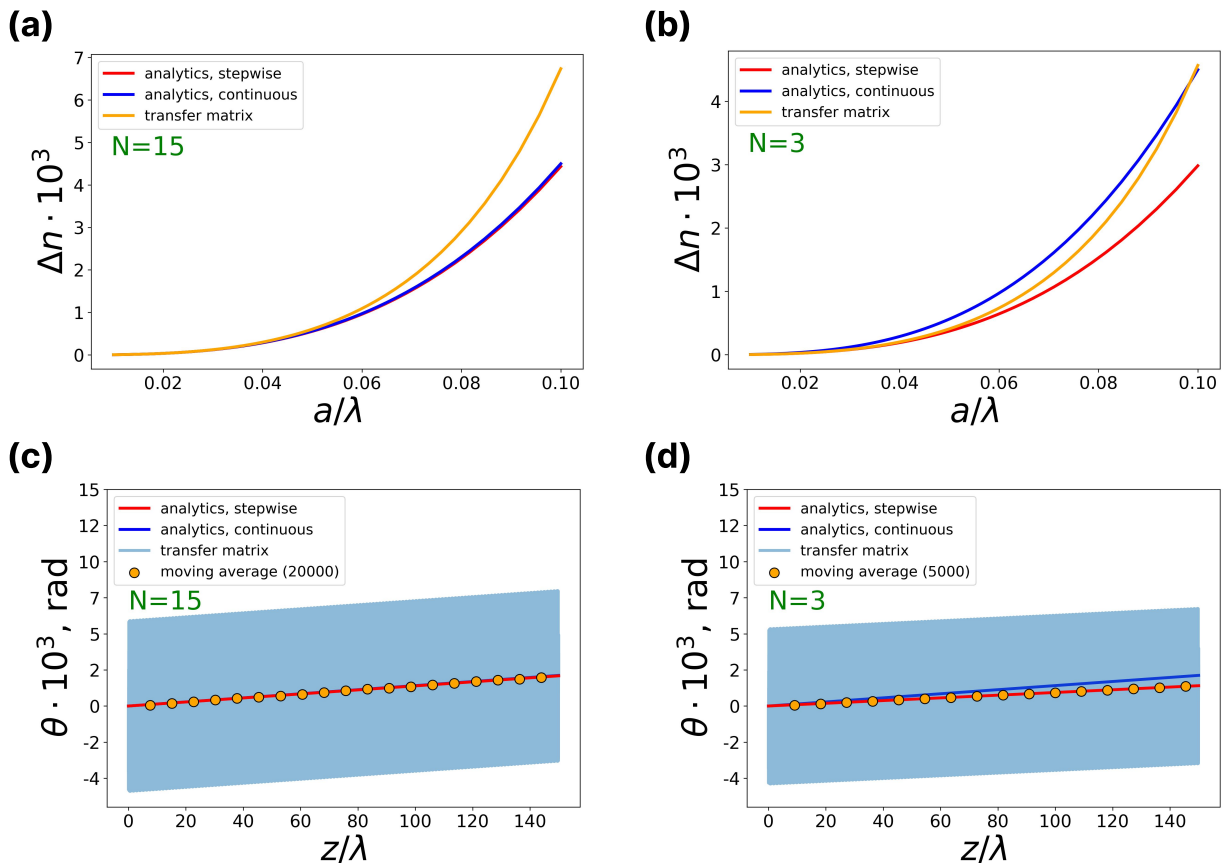


FIG. 3. Probing the eigenmodes of a multilayered structure composed of anisotropic layers. (a,b) Refractive index difference for the two forward-propagating modes versus a/λ ratio when the period consists of (a) $N = 15$ and (b) $N = 3$ layers, respectively. Orange, blue and red line depict the results of rigorous transfer matrix simulation and analytical calculation for the continuous and stepwise anisotropy axis rotation, respectively. (c,d) Polarization plane rotation for the linearly polarized wave propagating in the bulk metamaterial with $a/\lambda = 0.01$. Light blue line depicts the results of transfer matrix simulation, orange dots correspond to the moving average over 200 and 500 layers, 10 dots are taken within each layer. Blue and red curves show the analytical results for the continuous and stepwise rotation of anisotropy axis. The permittivity of the layers is $\epsilon_1 = 10$, $\epsilon_2 = 7$. The overall number of periods is equal to 15000.

quantifies the effective chirality [see Eq. (23)]. As chirality is proportional to $(a/\lambda)^3$, Δn is tiny in the deeply subwavelength region $\xi = a/\lambda \ll 1$. However, with the increase of ξ up to 0.06, Δn grows rapidly. At this point, the developed perturbation theory is no longer valid, and the discrepancy between the effective medium model and transfer matrix method mounts. At the same time, the assumption about the continuous rotation of anisotropy axis remains good approximation for $N = 15$ layers in the period.

A qualitatively similar behavior of Δn is observed, when the period of the lattice includes just $N = 3$ layers [Fig. 3(b)]. In this case, however, one has to take into account that the rotation of anisotropy axis from layer to layer is not continuous, but rather stepwise, as further analyzed in the Supplementary Materials, Sec. II.

Another aspect of chirality is the rotation of polarization plane of the linearly polarized wave propagating in the chiral medium. Decomposing the wave into two

circularly polarized modes and taking into account the difference of the refractive indices, Eq. (23), we recover the rotation $\theta = -q\kappa_{\text{eff}}z$. The results for $N = 15$ and $N = 3$ layers in the period for the fixed ratio $a/\lambda = 0.01$ are presented in Fig. 3(c,d). We compare these results with the transfer matrix calculation. In the latter case, however, polarization varies strongly within the layer, being elliptical in the general case. We compute the angle of rotation at each point as

$$\theta = \frac{1}{2} \arctan \left(\frac{2E_{tx}E_{ty} \cos(\Delta\phi)}{E_{tx}^2 - E_{ty}^2} \right),$$

where E_{tx} and E_{ty} are the amplitudes of light transmitted through each layer and $\Delta\phi$ is the phase difference between those components. These results are depicted by the thin blue line in Fig. 3(c,d) creating a uniform shading due to the rapid oscillations of polarization within the metamaterial period. Next we average the rotation angle taking a sliding averaging window. The obtained

averaged results are in full agreement with the analytical theory demonstrating the rotation of polarization plane linearly growing with distance indicating the onset of effective chirality.

V. MAXIMIZATION OF EFFECTIVE CHIRALITY

To illustrate the power of the obtained general solution for chirality κ_{eff} , we explore the following problem. Assume that the multilayered structure is composed of very thin layers with the given principal components of permittivity tensor ε_1 , ε_2 , and the period a of the lattice is fixed. In this setting, emergent chirality depends on the orientation of the layers described by the periodic function $\alpha(z)$. Below, we aim to find the arrangement of the layers maximizing chiral response κ_{eff} .

To do so, we compare Eqs. (13) and (15) and present chirality in the form

$$\kappa_{\text{eff}} \mathbf{e}_z^\times = i \frac{q^3}{b^3} \sum_{n \neq 0} \frac{1}{n^3} \hat{\varepsilon}_{-n} \hat{\varepsilon}_n. \quad (27)$$

For our analysis, it is convenient to transform Eq. (27) replacing the summation of the Fourier harmonics by the integration in the real space. Assuming that arbitrary periodic function $f(z)$ is presented in the form

$$f(z) = \sum_{n=-\infty}^{\infty} f_n e^{inbz}$$

we introduce the operator \mathcal{J} acting in the Fourier space as

$$(\mathcal{J}f)_n = \begin{cases} \frac{1}{ibn} f_n, & n \neq 0 \\ 0, & n = 0. \end{cases} \quad (28)$$

Essentially, this subtracts the average from the function $f(z)$, integrates it over the interval $[0, z]$ and subtracts the average from the resulting function. Accordingly, in the real space the operator \mathcal{J} acts as

$$\mathcal{J}f(z) = \int_0^a K_1 \left(\frac{z-z'}{a} \right) f(z') dz', \quad (29)$$

$$K_1(\xi) = \frac{1}{2} \text{sign}(\xi) - \xi. \quad (30)$$

Having Eq. (29), it is straightforward to compute the repeated action of the operator \mathcal{J} . For instance,

$$\mathcal{J}^3 f(z) = a^2 \int_0^a K_3 \left(\frac{z-z'}{a} \right) f(z') dz', \quad (31)$$

$$K_3(\xi) = -\frac{1}{12} \xi (1 - 3|\xi| + 2\xi^2). \quad (32)$$

Yet another ingredient needed for our calculation are the definitions of the scalar product and norm

$$\langle f, g \rangle = \int_0^a f^*(z) g(z) dz = a \sum_{n=-\infty}^{\infty} f_n^* g_n, \quad (33)$$

$$\|f\|^2 = \langle f, f \rangle = a \sum_{n=-\infty}^{\infty} |f_n|^2. \quad (34)$$

As the permittivity tensor of the layers is real, $\hat{\varepsilon}_{-n} = \hat{\varepsilon}_n^*$ and therefore

$$\begin{aligned} \kappa_{\text{eff}} \mathbf{e}_z^\times &= q^3 \sum_{n \neq 0} \hat{\varepsilon}_n^* \frac{\hat{\varepsilon}_n}{(ibn)^3} = q^3 \sum_{n \neq 0} \hat{\varepsilon}_n^* (\mathcal{J}^3 \hat{\varepsilon})_n \\ &= \frac{q^3}{a} \int_0^a \hat{\varepsilon}(z) [\mathcal{J}^3 \hat{\varepsilon}(z)] dz \\ &= q^3 a \int_0^a \int_0^a \hat{\varepsilon}(z) K_3 \left(\frac{z-z'}{a} \right) \hat{\varepsilon}(z') dz' dz \\ &= \frac{q^3 a}{2} \int_0^a \int_0^a K_3 \left(\frac{z-z'}{a} \right) [\hat{\varepsilon}(z), \hat{\varepsilon}(z')] dz' dz. \end{aligned} \quad (35)$$

Straightforward calculation of the commutator using Eq. (7) yields

$$[\hat{\varepsilon}(z), \hat{\varepsilon}(z')] = 2\Delta\varepsilon^2 \text{Im} \left(e^{2i\alpha(z)} e^{-2i\alpha(z')} \right) \mathbf{e}_z^\times \quad (36)$$

giving an explicit formula for chirality

$$\begin{aligned} \kappa_{\text{eff}} &= q^3 a \Delta\varepsilon^2 \text{Im} \int_0^a \int_0^a K_3 \left(\frac{z-z'}{a} \right) e^{2i\alpha(z)} e^{-2i\alpha(z')} dz dz' \\ &= \frac{q^3}{a} \Delta\varepsilon^2 \text{Im} \langle \psi, \mathcal{J}^3 \psi \rangle, \end{aligned} \quad (37)$$

where $\psi(z) = \exp(-2i\alpha(z))$ is an auxiliary scalar function. The latter expression can be readily estimated as follows:

$$\begin{aligned} |\text{Im} \langle \psi, \mathcal{J}^3 \psi \rangle| &= a \left| \text{Im} \sum_{n \neq 0} \frac{\psi_n^* \psi_n}{-ib^3 n^3} \right| \\ &\leq \frac{a}{b^3} \sum_{n \neq 0} \left| \frac{1}{n^3} \right| \psi_n^* \psi_n \leq \frac{a}{b^3} \sum_n \psi_n^* \psi_n \\ &= \frac{1}{b^3} \|\psi\|^2 = \frac{a}{b^3} \end{aligned}$$

Hence, an upper bound for chirality κ_{eff} reads:

$$|\kappa_{\text{eff}}| \leq \frac{q^3}{b^3} \Delta\varepsilon^2. \quad (38)$$

This value is achieved for $\psi = e^{-ibz}$. Thus, we conclude that the arrangement of the layers maximizing chiral response is the continuous rotation of anisotropy axis, i.e. spiral symmetry.

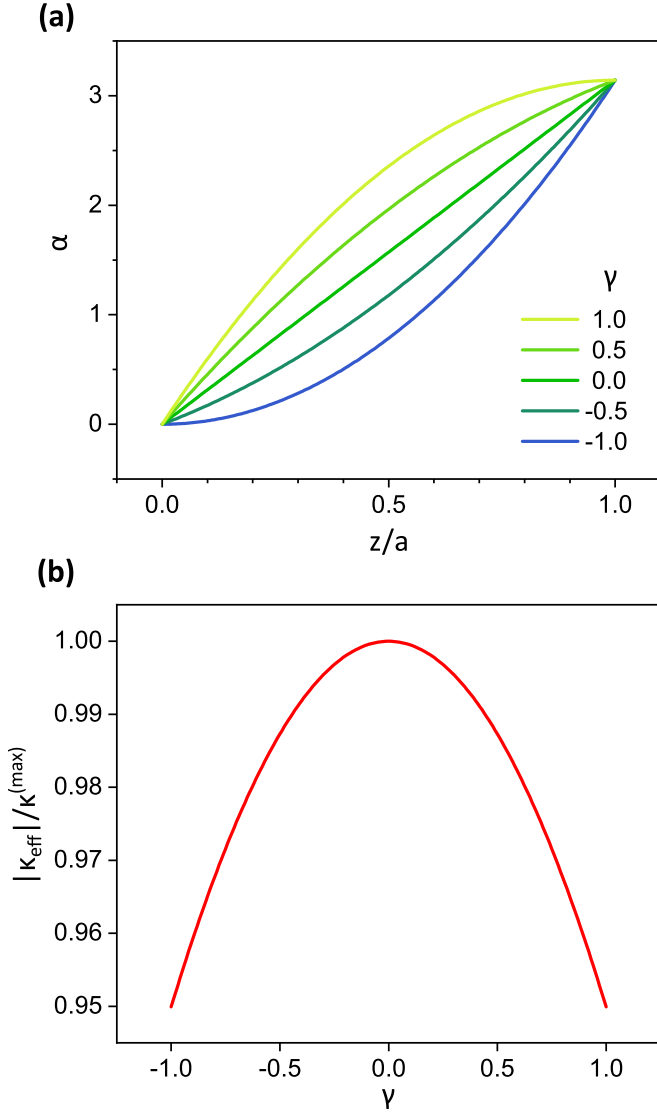


FIG. 4. Illustration of effective chirality maximization. (a) Various laws of anisotropy axis rotation $\alpha(z)$ distinguished by the γ parameter. (b) Relative effective chirality as a function of γ . Chirality reaches its maximum for the uniform rotation of anisotropy axis, i.e. in case of spiral symmetry.

To illustrate that, we chose a specific set of $\alpha(z)$ functions, parameterized by γ as follows:

$$\alpha_\gamma(z) = \pi \left[\frac{z}{a} + \gamma \frac{z}{a} \left(1 - \frac{z}{a} \right) \right] \quad (39)$$

In Fig. 4 we plot the dependence of effective chirality κ_{eff} on γ . We chose a range $[-1, 1]$ for γ , so that the rotation angle $\alpha(z)$ changes monotonously with z . As anticipated from our general analysis, chiral response reaches its maximum exactly for $\gamma = 0$.

VI. RECONSTRUCTION OF THE FULL CHIRALITY TENSOR

In this section, we generalize our treatment and examine an arbitrary direction of \mathbf{k} vector. In experimental situation, this corresponds to the oblique incidence scenario. For simplicity, we assume that the anisotropy axis rotates continuously according to Eq. (2), so that the effective chirality tensor has the diagonal structure, Eq. (4). While κ_{11} component is calculated above, κ_{33} term is only manifested at oblique incidence.

As we consider an unbounded medium with spiral symmetry, without loss of generality we can rotate the coordinate system and assume that the wave vector is $\mathbf{k} = (k_x, 0, k_z)^\top$, while all components of electric field are nonzero $\mathbf{E} = (E_x, E_y, E_z)^\top$. In such setting, the wave equation Eq. (9) results in the system:

$$-(k_z + nb)^2 E_{nx} + k_x(k_z + nb)E_{nz} + q^2 D_{nx} = 0, \quad (40)$$

$$k_x(k_z + nb)E_{nx} - k_x^2 E_{nz} + q^2 D_{nz} = 0, \quad (41)$$

$$-(k_z + nb)^2 E_{ny} - k_x^2 E_{ny} + q^2 D_{ny} = 0. \quad (42)$$

Equations (40) and (41) can be combined to yield

$$k_x D_{nx} + (k_z + nb)D_{nz} = 0. \quad (43)$$

In turn, the material equation for the Floquet harmonics of electric field reads

$$\mathbf{D}_n = \sum_m \hat{\epsilon}_{n-m} \mathbf{E}_m, \quad (44)$$

or, alternatively, introducing the inverse permittivity $\hat{\zeta}$,

$$\mathbf{E}_n = \sum_m \hat{\zeta}_{n-m} \mathbf{D}_m. \quad (45)$$

Next we employ the perturbation theory with the small parameter $\xi = a/\lambda$ presenting the Floquet harmonics with $n \neq 0$ as a series

$$\begin{cases} E_{ni} = E_{ni}^{(0)} + \xi E_{ni}^{(1)} + \xi^2 E_{ni}^{(2)} + \dots \\ D_{ni} = D_{ni}^{(0)} + \xi D_{ni}^{(1)} + \xi^2 D_{ni}^{(2)} + \dots \end{cases} \quad (46)$$

where index $i = x, y, z$ labels the Cartesian component.

Performing the calculations similarly to the normal incidence case (see details in Supplementary Materials, Section III), we recover the effective material parameters:

$$\hat{\epsilon}_{\text{eff}} = \begin{pmatrix} \bar{\epsilon} + \frac{\Delta \epsilon^2}{2b^2} \left(2q^2 - \frac{k_x^2}{\epsilon_3} \right) & 0 & 0 \\ 0 & \bar{\epsilon} + \frac{\Delta \epsilon^2}{2b^2} \left(2q^2 - \frac{k_x^2}{\epsilon_3} \right) & 0 \\ 0 & 0 & \epsilon_3 \end{pmatrix},$$

$$\hat{\kappa}_{\text{eff}} = -\frac{q \Delta \epsilon^2}{2 b^3} \left(2q^2 - \frac{k_x^2}{\epsilon_3} \right) \begin{pmatrix} 1 & 0 & 0 \\ 0 & 1 & 0 \\ 0 & 0 & -1 \end{pmatrix}. \quad (47)$$

Interestingly, effective permittivity tensor $\hat{\varepsilon}_{\text{eff}}$ acquires second-order spatial dispersion correction, while effective chirality is cubic in ξ and also contains spatial dispersion contribution. Equation (47) suggests that κ_{33} component is nonzero and has different sign compared to κ_{11} .

To validate such behavior of effective chiral response, we analyze both refractive indices and polarizations of the modes supported by the structure at oblique incidence.

First, we fix the frequency $q = \omega/c$ and calculate the isofrequency contour in the Oxz plane. To isolate the effects due to chirality and spatial dispersion, we subtract from the propagation constant k_z its dominant part $k_z^{(u)}$ – a value obtained for a uniaxial non-chiral crystal with

$$\hat{\varepsilon}^{(u)} = \text{diag}(\bar{\varepsilon}, \bar{\varepsilon}, \varepsilon_3), \quad \hat{\kappa}^{(u)} = \hat{0}. \quad (48)$$

Figure 5(a) shows the corrections to the propagation constants of two forward-propagating ($k_z > 0$) modes at different incidence angles quantified by the k_x . We observe that the effective medium model correctly reproduces k_z values at all incidence angles.

To support our effective medium model further, we calculate the polarizations of the same modes quantifying them by the Stokes parameters defined as

$$S_0 = |E_{0x'}|^2 + |E_{0y'}|^2, \quad (49)$$

$$S_1 = |E_{0x'}|^2 - |E_{0y'}|^2, \quad (50)$$

$$S_2 = 2 \text{Re}(E_{0x'} E_{0y'}^*), \quad (51)$$

$$S_3 = -2 \text{Im}(E_{0x'} E_{0y'}^*). \quad (52)$$

Here, \mathbf{E}_0 denotes the averaged field calculated as

$$\mathbf{E}_0 = \frac{1}{a} \int_0^a \mathbf{E}(z) e^{-ik_z z} dz,$$

and k_z is recovered from the eigenmode calculation, Eq.(26). The Stokes parameters are evaluated in the plane $Ox'y'$ spanned by $\text{Re} \mathbf{E}_0$ and $\text{Im} \mathbf{E}_0$ vectors; Ox' corresponds to the projection of Ox axis onto the polarization plane, while Oy' axis satisfies the conditions

$$[\mathbf{e}_{x'} \times \mathbf{e}_{y'}] \cdot \mathbf{e}_z > 0, \quad \mathbf{e}_{x'} \cdot \mathbf{e}_{y'} = 0.$$

This choice of the coordinate system ensures that $S_2 = 0$.

In our calculation, we choose $\varepsilon_3 = \bar{\varepsilon}$ in order to mitigate the effect of optical anisotropy in the limit $\xi \rightarrow 0$ and isolate the influence of κ_{33} chirality component. We perform the effective medium calculation for various k_x and for the set of chirality tensors with different values of κ_{33} component: $\kappa_{33} = -s \kappa_{11}$ comparing the results for a mode with a larger k_z in Fig. 5(b,c). Comparing the analytical results with the transfer matrix calculation, we recover that the best approximation corresponds to $s = 1$, meaning that $\kappa_{33} = -\kappa_{11}$ in agreement with the theoretical prediction.

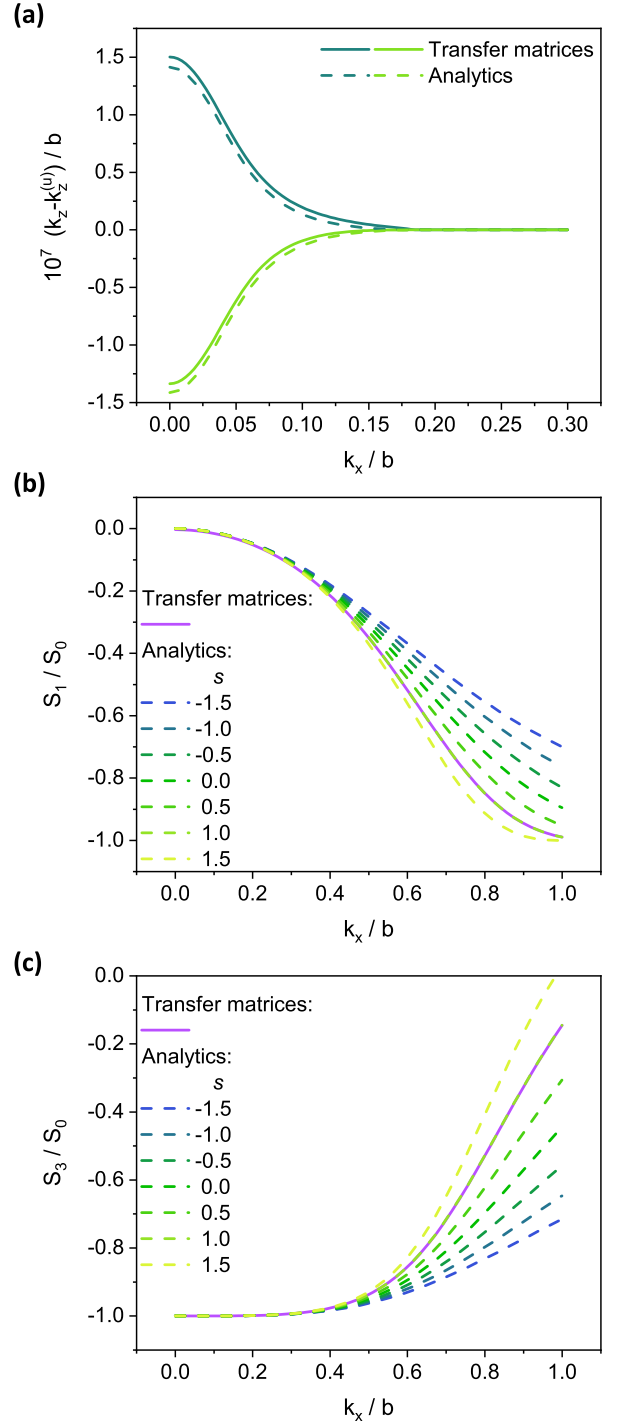


FIG. 5. Validation of effective medium description at oblique incidence. (a) Isofrequency contour in Oxz plane with $k_z^{(u)}$ for a uniaxial crystal subtracted. $a/\lambda = 0.01$ is fixed, the permittivity values for a single layer are $\varepsilon_1 = 10.0$, $\varepsilon_2 = 7.0$, $\varepsilon_3 = 8.5$. (b, c) Stokes parameters for a single eigenmode with the larger k_z , calculated by the transfer matrix method, superposed with analytical results corresponding to different values of κ_{33} . $a/\lambda = 0.06$, layer permittivities are the same as above.

VII. DISCUSSION AND CONCLUSIONS

In summary, we have derived a complete effective medium description of the multilayered structure composed of anisotropic layers rotated relative to each other. Our description captures the metamaterial regime when the lattice period is much smaller than the wavelength. In such case, electromagnetic chirality is proportional to $(a/\lambda)^3$ and features spatial dispersion contribution at oblique incidence.

As we proved, continuous rotation of anisotropy axis from layer to layer maximizes the effective chirality compared to any other configuration with the same lattice period a and permittivities of the individual layers ε_1 and ε_2 .

While our analysis provides insights into the emergence of effective chirality in a stack of anisotropic layers, we

believe that our methodology is more general and enables understanding of other layered geometries featuring more exotic responses. It could also pave a way to the reverse engineering of metamaterial structures with the prescribed effective properties.

ACKNOWLEDGMENTS

We acknowledge Daniel Bobylev for valuable discussions. Theoretical models were supported by the Russian Science Foundation (grant No. 23-72-10026). Numerical investigation of the structure was supported by the Russian Science Foundation (grant No. 24-72-10069). Analysis of chiral response maximization was supported by Priority 2030 Federal Academic Leadership Program. M.A.G. acknowledges partial support from the Foundation for the Advancement of Theoretical Physics and Mathematics “Basis”.

-
- [1] V. G. Veselago, The electrodynamics of substances with simultaneously negative values of ϵ and μ , *Soviet Physics Uspekhi* **10**, 509 (1968).
 - [2] G. V. Eleftheriades and K. G. Balmain, *Negative-Refraction Metamaterials: Fundamental Principles and Applications* (John Wiley & Sons, New Jersey, 2005).
 - [3] R. Marques, F. Martin, and M. Sorolla, *Metamaterials with negative parameters* (John Wiley & Sons, New Jersey, 2008).
 - [4] V. I. Belotelov, L. L. Doskolovich, and A. K. Zvezdin, Extraordinary Magneto-Optical Effects and Transmission through Metal-Dielectric Plasmonic Systems, *Physical Review Letters* **98**, 077401 (2007).
 - [5] V. S. Asadchy, A. Díaz-Rubio, and S. A. Tretyakov, Bianisotropic metasurfaces: physics and applications, *Nanophotonics* **7**, 1069 (2018).
 - [6] P. A. Belov, R. Marqués, S. I. Maslovski, I. S. Nefedov, M. Silveirinha, C. R. Simovski, and S. A. Tretyakov, Strong spatial dispersion in wire media in the very large wavelength limit, *Physical Review B* **67**, 113103 (2003).
 - [7] A. A. Orlov, P. M. Voroshilov, P. A. Belov, and Y. S. Kivshar, Engineered optical nonlocality in nanostructured metamaterials, *Physical Review B* **84**, 045424 (2011).
 - [8] L. Shaposhnikov, M. Mazanov, D. A. Bobylev, F. Wilczek, and M. A. Goralch, Emergent axion response in multilayered metamaterials, *Physical Review B* **108**, 115101 (2023).
 - [9] S. Safaei Jazi, I. Faniayeu, R. Cicheler, D. C. Tzarouchis, M. M. Asgari, A. Dmitriev, S. Fan, and V. Asadchy, Optical Tellegen metamaterial with spontaneous magnetization, *Nature Communications* **15**, 1293 (2024).
 - [10] B. Semnani, J. Flannery, R. Al Maruf, and M. Bajcsy, Spin-preserving chiral photonic crystal mirror, *Light: Science & Applications* **9**, 23 (2020).
 - [11] K. Voronin, A. S. Taradin, M. V. Gorkunov, and D. G. Baranov, Single-Handedness Chiral Optical Cavities, *ACS Photonics* **9**, 2652 (2022).
 - [12] D. G. Baranov, C. Schäfer, and M. V. Gorkunov, Toward Molecular Chiral Polaritons, *ACS Photonics* **10**, 2440 (2023).
 - [13] Y. Tang and A. E. Cohen, Optical Chirality and Its Interaction with Matter, *Physical Review Letters* **104**, 163901 (2010).
 - [14] I. Fernandez-Corbaton, M. Fruhnert, and C. Rockstuhl, Objects of Maximum Electromagnetic Chirality, *Physical Review X* **6**, 031013 (2016).
 - [15] W. Chen, Z. Wang, M. V. Gorkunov, J. Qin, R. Wang, C. Wang, D. Wu, J. Chu, X. Wang, Y. Kivshar, and Y. Chen, Uncovering Maximum Chirality in Resonant Nanostructures, *Nano Letters* **24**, 9643 (2024).
 - [16] A. Serdyukov, I. Semchenko, S. Tretyakov, and A. Sihvola, *Electromagnetics of Bi-anisotropic Materials: Theory and Applications* (Gordon and Breach Science Publishers, Amsterdam, 2001).
 - [17] X. Yin, M. Schäferling, B. Metzger, and H. Giessen, Interpreting Chiral Nanophotonic Spectra: The Plasmonic Born–Kuhn Model, *Nano Letters* **13**, 6238 (2013).
 - [18] L. Barron, *Molecular Light Scattering and Optical Activity*, 2nd ed. (Cambridge University Press, Cambridge, UK, 2004).
 - [19] S. Y. Vetrov, I. V. Timofeev, and V. F. Shabanov, Localized modes in chiral photonic structures, *Physics-Uspekhi* **63**, 33 (2020).
 - [20] L. Rebholz, M. Krstić, B. Zerulla, M. Pawlak, W. Lewandowski, I. Fernandez-Corbaton, and C. Rockstuhl, Separating the Material and Geometry Contribution to the Circular Dichroism of Chiral Objects Made from Chiral Media, *ACS Photonics* **11**, 1771 (2024).
 - [21] P. G. de Gennes and J. Prost, *The Physics of Liquid Crystals* (Clarendon Press, Oxford, England, UK, 1993).
 - [22] I.-C. Khoo, *Liquid Crystals, 3rd Edition* (Wiley, Hoboken, NJ, USA, 2022).
 - [23] K. V. Voronin, A. N. Toksumakov, G. A. Ermolaev, A. S. Slavich, M. K. Tatmyshevskiy, S. M. Novikov, A. A.

- Vyshnevyy, A. V. Arsenin, K. S. Novoselov, D. A. Ghazaryan, *et al.*, Chiral Photonic Super-Crystals Based on Helical van der Waals Homostructures, *Laser & Photonics Reviews* **18**, 2301113 (2024).
- [24] M. G. Silveirinha, Metamaterial homogenization approach with application to the characterization of microstructured composites with negative parameters, *Physical Review B* **75**, 115104 (2007).
- [25] M. A. Gorlach and M. Lapine, Boundary conditions for the effective-medium description of subwavelength multilayered structures, *Physical Review B* **101**, 075127 (2020).

Supplemental Materials: Effective chiral response of anisotropic multilayered metamaterials

Konstantin Baranov,^{1,*} Dmitry Vagin,^{1,*} and Maxim A. Gorlach^{1,†}

¹*School of Physics and Engineering, ITMO University, Saint Petersburg 197101, Russia*

CONTENTS

I. Polarization and refractive indices of the eigenmodes in a helicoidal medium	1
II. Derivation of non-zero Fourier components of permittivity tensor for the case of normal incidence and its analysis	4
A. Derivation of non-zero Fourier components of the dielectric permittivity tensor	4
B. Calculation of sums with commutative and anticommutative relations	7
III. Derivation of the full chirality tensor	8
A. Zero and first order of perturbation theory	10
B. Second order of perturbation theory	11
C. Third order of perturbation theory	13
D. Reducing the material equations to canonical bianisotropic form	15
References	17

I. POLARIZATION AND REFRACTIVE INDICES OF THE EIGENMODES IN A HELICOIDAL MEDIUM

In this section, we revisit the problem of light propagation in a dielectric medium with spiral symmetry, i.e. the medium invariant under the combination of infinitesimal rotation and the proportional translation. We treat this problem analogously to Refs. [1, 2] generalizing the approach to the arbitrary local material of the layers and computing the refractive indices of the eigenmodes and their polarizations.

We start with Maxwell's equations in a monochromatic case and in the absence of sources written in the CGS system of units

$$\begin{cases} \nabla \times \mathbf{E} = iq\mathbf{B}, \\ \nabla \times \mathbf{H} = -iq\mathbf{D}, \\ \nabla \cdot \mathbf{D} = 0, \\ \nabla \cdot \mathbf{B} = 0, \end{cases} \quad (\text{S1})$$

where $q = \omega/c$. If the fields change strictly along Oz axis, i.e. normal incidence scenario is realized, then

$$\begin{cases} \mathbf{e}_z \times \partial_z \mathbf{E} = iq\mathbf{B}, \\ \mathbf{e}_z \times \partial_z \mathbf{H} = -iq\mathbf{D}, \\ \mathbf{e}_z \cdot \partial_z \mathbf{D} = 0, \\ \mathbf{e}_z \cdot \partial_z \mathbf{B} = 0. \end{cases} \quad (\text{S2})$$

* These authors have contributed equally to this work

† m.gorlach@metalab.ifmo.ru

The full system of equations governing the evolution of the fields is composed of Maxwell's equations Eq. (S2) and the system of constitutive relations, generally written as

$$\begin{cases} \mathbf{D} = \hat{\epsilon}\mathbf{E} + \hat{\alpha}\mathbf{H} \\ \mathbf{B} = \hat{\beta}\mathbf{E} + \hat{\mu}\mathbf{H}, \end{cases} \quad (\text{S3})$$

where $\hat{\epsilon}$, $\hat{\mu}$, $\hat{\alpha}$ and $\hat{\beta}$ denote local material parameters. Next we introduce a 6-component vector of electric and magnetic fields constructing it from the components continuous at the boundary between the different media:

$$\mathbf{F} = (E_x, E_y, D_z, H_x, H_y, B_z)^T, \quad (\text{S4})$$

and obtain the first-order differential equation

$$\partial_z \mathbf{F} = -i\hat{\mathcal{T}}\mathbf{F} \quad (\text{S5})$$

with matrix $\hat{\mathcal{T}}$ expressed via the coefficients of $\hat{\epsilon}$, $\hat{\mu}$, $\hat{\alpha}$, $\hat{\beta}$. While general expression for $\hat{\mathcal{T}}$ is cumbersome, the result for anisotropic layer with the permittivity tensor $\hat{\epsilon} = \text{diag}(\epsilon_1, \epsilon_2, \epsilon_3)$ is readily recovered from Eq. (S2) and reads

$$\hat{\mathcal{T}}_{\text{loc}} = q \begin{pmatrix} 0 & 0 & 0 & 0 & -1 & 0 \\ 0 & 0 & 0 & 1 & 0 & 0 \\ 0 & 0 & 0 & 0 & 0 & 0 \\ 0 & \epsilon_2 & 0 & 0 & 0 & 0 \\ -\epsilon_1 & 0 & 0 & 0 & 0 & 0 \\ 0 & 0 & 0 & 0 & 0 & 0 \end{pmatrix} \quad (\text{S6})$$

Physically, $\hat{\mathcal{T}}$ matrix provides a generator of translations along the z axis and embeds all the relevant properties of the medium under study. Accordingly, the values of \mathbf{F} at two close points are related as

$$\mathbf{F}(z + dz) = (1 - i dz \mathcal{T}(z)) \mathbf{F}(z).$$

By construction, the object F transforms as a direct sum of two vectors under rotations $\hat{R}(\theta)$ around z axis:

$$F' = \begin{pmatrix} \hat{R}(\theta) & 0 \\ 0 & \hat{R}(\theta) \end{pmatrix} F = \hat{R}^{(2)}(\theta) F,$$

where the rotation matrix is given by

$$\hat{R}(\alpha) = \begin{pmatrix} \cos \theta & -\sin \theta & 0 \\ \sin \theta & \cos \theta & 0 \\ 0 & 0 & 1 \end{pmatrix}. \quad (\text{S7})$$

In a similar manner to $\hat{\mathcal{T}}$, we introduce $\hat{\mathcal{R}}$ – a generator of infinitesimal $\hat{R}^{(2)}$ rotation:

$$\hat{R}^{(2)}(\theta + d\theta) = (\hat{I} + i d\theta \hat{\mathcal{R}}) \hat{R}^{(2)}(\theta). \quad (\text{S8})$$

Explicit calculation yields

$$\hat{\mathcal{R}} = \begin{pmatrix} 0 & i & 0 & 0 & 0 & 0 \\ -i & 0 & 0 & 0 & 0 & 0 \\ 0 & 0 & 0 & 0 & 0 & 0 \\ 0 & 0 & 0 & 0 & i & 0 \\ 0 & 0 & 0 & -i & 0 & 0 \\ 0 & 0 & 0 & 0 & 0 & 0 \end{pmatrix}. \quad (\text{S9})$$

As $\hat{\mathcal{R}}$ is independent of θ , the rotation for the arbitrary angle θ can be written as

$$\hat{R}^{(2)}(\theta) = \exp(i\theta \hat{\mathcal{R}}). \quad (\text{S10})$$

Now we utilize the symmetry of the structure. Spiral symmetry of the medium implies that its properties are invariant under dz translation accompanied by $d\theta = \pi dz/a = bdz/2$ rotation. Technically, this means that the generator $\hat{\mathcal{T}}(z)$ capturing the properties of the medium depends on z as follows:

$$\hat{\mathcal{T}}(z) = \hat{R}^{(2)}(bz/2) \hat{\mathcal{T}}_{\text{loc}} \hat{R}^{(2)}(-bz/2), \quad (\text{S11})$$

where $\hat{\mathcal{T}}_{\text{loc}} = \hat{\mathcal{T}}(0)$. Our goal now is to solve the differential equation Eq. (S5) with the z -dependent translation generator \mathcal{T} given by Eq. (S11). To do this, we consider the fields in a local coordinate system, i.e. the coordinate system associated with the principal axes of the respective layer:

$$\mathbf{F}_{\text{loc}} = \hat{R}^{(2)}(-bz/2)\mathbf{F}. \quad (\text{S12})$$

Next, we derive the differential equation for \mathbf{F}_{loc} :

$$\begin{aligned} \partial_z \mathbf{F}_{\text{loc}} &= \left(\partial_z \hat{R}^{(2)}(-bz/2) \right) \mathbf{F} + \hat{R}^{(2)}(-bz/2) \partial_z \mathbf{F} \\ &= -i \frac{b}{2} \hat{\mathcal{R}} \hat{R}^{(2)}(-bz/2) \mathbf{F} - \hat{R}^{(2)}(-bz/2) i \hat{\mathcal{T}}(z) \mathbf{F} \\ &= -i \frac{b}{2} \hat{\mathcal{R}} \hat{R}^{(2)}(-bz/2) \mathbf{F} - i \hat{\mathcal{T}}_{\text{loc}} \hat{R}^{(2)}(-bz/2) \mathbf{F} \end{aligned} \quad (\text{S13})$$

Thus, we recover that the fields in a local coordinate frame satisfy the differential equation with constant coefficients:

$$\partial_z \mathbf{F}_{\text{loc}} = -i \left(\hat{\mathcal{T}}_{\text{loc}} + \frac{b}{2} \hat{\mathcal{R}} \right) \mathbf{F}_{\text{loc}} \quad (\text{S14})$$

The solution to this differential equation is a matrix exponent

$$\mathbf{F}_{\text{loc}}(z) = \exp \left\{ -iz \left(\hat{\mathcal{T}}_{\text{loc}} + \frac{b}{2} \hat{\mathcal{R}} \right) \right\} \mathbf{F}(0), \quad \mathbf{F}(z) = \exp \left\{ iz \frac{b}{2} \hat{\mathcal{R}} \right\} \exp \left\{ -iz \left(\hat{\mathcal{T}}_{\text{loc}} + \frac{b}{2} \hat{\mathcal{R}} \right) \right\} \mathbf{F}(0). \quad (\text{S15})$$

Equation (S15) now allows to compute the eigenmodes of the medium. Periodicity of the metamaterial guarantees that there is a basis of solutions satisfying $\mathbf{F}(z+a) = \mathbf{F}(z) e^{ik_a}$, where k is the Bloch wave number related to the effective refractive index as $k = qn$. These Bloch modes are the eigenvectors of $\hat{\mathcal{T}}_{\text{loc}} + \frac{b}{2} \hat{\mathcal{R}}$. Indeed, if $\tilde{\mathbf{F}}_j$ satisfies

$$\left(\hat{\mathcal{T}}_{\text{loc}} + \frac{b}{2} \hat{\mathcal{R}} \right) \tilde{\mathbf{F}}_j = \lambda_j \tilde{\mathbf{F}}_j$$

then by substituting $\mathbf{F}(0) = \tilde{\mathbf{F}}_j$ into Eq. (S15) we obtain

$$\mathbf{F}(a) = \hat{R}^{(2)}(\pi) e^{-i\lambda_j a} \mathbf{F}(0) \quad (\text{S16})$$

and recover the refractive index of every mode up to a multiple of $2\pi/(qa)$:

$$qn_j = -\lambda_j + \frac{\pi - 2\pi l}{a}, \quad (\text{S17})$$

where l is an arbitrary integer. The limit at $\xi \rightarrow 0$, where $\xi = q/b$, allows us to resolve the ambiguity. In this limit $qn_j \rightarrow 0$ and therefore

$$qn_j(\xi) = -\lambda_j(\xi) + \lim_{\xi' \rightarrow 0} \lambda_j(\xi'). \quad (\text{S18})$$

We note that $\lim_{\xi' \rightarrow 0} \lambda_j(\xi')$ are eigenvalues of $\frac{b}{2} \hat{\mathcal{R}}$, meaning those can be represented as multiples of π/a , showing consistency between Eq. (S17) and Eq. (S18). By applying Eq. (S18) to the stack of anisotropic dielectric layers, described in the main text of this Article, we find two refractive indices for forward-propagating ($k > 0$) modes:

$$n_{\pm} = \frac{b - \sqrt{-4q\sqrt{b^2\bar{\epsilon}} + \Delta\epsilon^2 q^2 + b^2 + 4q^2\bar{\epsilon}}}{2q}, \quad n_{\pm} = \frac{\sqrt{4q\sqrt{b^2\bar{\epsilon}} + \Delta\epsilon^2 q^2 + b^2 + 4q^2\bar{\epsilon}} - b}{2q}, \quad (\text{S19})$$

where $\bar{\epsilon} = (\epsilon_1 + \epsilon_2)/2$ and $\Delta\epsilon = (\epsilon_2 - \epsilon_1)/2$ as in the main text. A simple series expansion yields

$$n_{\pm} = \sqrt{\epsilon_0} + \frac{\Delta\epsilon^2 q^2}{2b^2 \sqrt{\epsilon_0}} \mp \frac{\Delta\epsilon^2 q^3}{b^3} + O(\xi^4).$$

When compared with the dispersion relation in chiral medium

$$n_{\pm} = \sqrt{\epsilon_{\text{eff}}} \pm \kappa_{\text{eff}},$$

this allows us to evaluate the effective material parameters:

$$\varepsilon_{\text{eff}} = \bar{\varepsilon} + \frac{\Delta\varepsilon^2 q^2}{b^2} + O(\xi^3), \quad \kappa_{\text{eff}} = -\frac{\Delta\varepsilon^2 q^3}{b^3} + O(\xi^4). \quad (\text{S20})$$

These values precisely match those obtained in the main text via rigorous homogenization approach. To consistently determine the sign of chirality in Eq. (S20), we consider the averaged field of each eigenmode, calculating

$$\mathbf{F}_0 = \frac{1}{a} \int_0^a \mathbf{F}(z) e^{-inqz} dz. \quad (\text{S21})$$

This is easily accomplished by decomposing $\hat{\mathcal{R}}$ into a linear combination of projection matrices and rewriting Eq. (S15) with $\mathbf{F}(0) = \tilde{\mathbf{F}}_j$:

$$\begin{aligned} \hat{\mathcal{R}} &= \sum_l \mu_l \hat{P}_l, \quad \hat{P}_l^2 = \hat{P}_l, \quad \sum_l \hat{P}_l = \hat{I}. \\ \mathbf{F}(z) &= \sum_l \exp\left\{iz \frac{b}{2} \mu_l\right\} \hat{P}_l \exp\{-iz \lambda_j\} \tilde{\mathbf{F}}_j \\ \mathbf{F}_0^{(j)} &= \sum_l \left(\frac{1}{a} \int_0^a \exp\left\{iz \frac{b}{2} \mu_l - iz \lim_{\xi \rightarrow 0} \lambda_j(\xi)\right\} \right) \hat{P}_l \tilde{\mathbf{F}}_j \end{aligned} \quad (\text{S22})$$

In the latter equation the value of refractive index is substituted from Eq. (S18). Only one summand in Eq. (S22) remains for each j . We denote its index by l_j , so that

$$i \frac{b}{2} \mu_{l_j} - i \lim_{\xi \rightarrow 0} \lambda_j(\xi) = 0.$$

The final expression:

$$\mathbf{F}_0^{(j)} = \hat{P}_{l_j} \tilde{\mathbf{F}}_j \quad (\text{S23})$$

Projection matrices \hat{P}_{l_j} filter out either one of two circularly polarized waves or a longitudinal wave. We identify that in Eq. (S19) n_+ corresponds to the right-handed circularly polarized mode and n_- corresponds to the left-handed one. While local fields $\mathbf{F}(z)$ are elliptically polarized, homogenized modes are polarized circularly. This result is general, the equation (S23) does not depend on local constitutive relations, but rather follows from the symmetry of the arrangement.

The procedure described above is applicable to the case of oblique incidence as well. However simple analytical solutions, arising due to the constant coefficients in Eq. (S14), are no longer available. The local translation generator in this case reads

$$\hat{\mathcal{T}}_{\text{loc}} = \begin{pmatrix} 0 & 0 & -\frac{k_{\text{loc},x}}{\varepsilon_3} & 0 & -q & 0 \\ 0 & 0 & -\frac{k_{\text{loc},y}}{\varepsilon_3} & q & 0 & 0 \\ k_{\text{loc},x} \varepsilon_1 & k_{\text{loc},y} \varepsilon_2 & 0 & 0 & 0 & 0 \\ 0 & q\varepsilon_2 & 0 & 0 & 0 & -k_{\text{loc},x} \\ -q\varepsilon_1 & 0 & 0 & 0 & 0 & -k_{\text{loc},y} \\ 0 & 0 & 0 & k_{\text{loc},x} & k_{\text{loc},y} & 0 \end{pmatrix}$$

where \mathbf{k}_{loc} is defined as

$$\mathbf{k}_{\text{loc}} = \hat{R}(-bz/2) \mathbf{k}.$$

II. DERIVATION OF NON-ZERO FOURIER COMPONENTS OF PERMITTIVITY TENSOR FOR THE CASE OF NORMAL INCIDENCE AND ITS ANALYSIS

A. Derivation of non-zero Fourier components of the dielectric permittivity tensor

Fourier components can be written in the following form

$$\hat{\varepsilon}_n = \frac{1}{a} \int_0^a \hat{\varepsilon}(z) e^{-inbz} dz = \frac{1}{a} \left[\int_0^a \bar{\varepsilon} \hat{I} e^{-inbz} dz + \Delta\varepsilon \int_0^a \begin{pmatrix} -\cos(2\alpha) & -\sin(2\alpha) \\ -\sin(2\alpha) & \cos(2\alpha) \end{pmatrix} e^{-inbz} dz \right]. \quad (\text{S24})$$

First integral in the right hand side of (S24) vanishes, if $n \neq 0$

$$\int_0^a \bar{\varepsilon} \hat{I} e^{-inbz} dz = \begin{cases} \bar{\varepsilon} \hat{I} a, & n = 0 \\ 0, & n \neq 0 \end{cases}. \quad (\text{S25})$$

Since the angle α , describing the rotation of the anisotropy axis, has period π , for the m -th layer it is determined as

$$\alpha_m = \frac{\pi(m-1)}{N}, \quad (\text{S26})$$

where N is the number of layers in the period, $m \geq 1$.

Fig. S1 shows the dependence of anisotropy axis rotation from layer to layer on the thickness of multilayer structure.

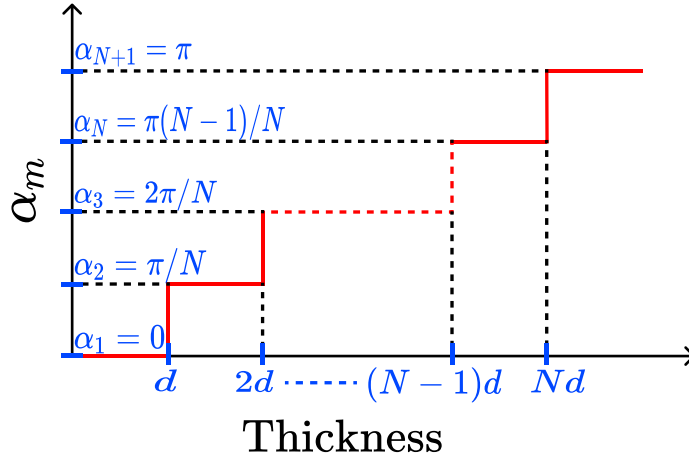


FIG. S1. The illustration of the stepwise anisotropy axis rotation

Now the second integral from equation (S24), containing the angle α in the argument of the trigonometric functions, can be divided into N integrals:

$$\begin{aligned} \int_0^a \begin{pmatrix} -\cos(2\alpha) & -\sin(2\alpha) \\ -\sin(2\alpha) & \cos(2\alpha) \end{pmatrix} e^{-inbz} dz &= \int_0^d \begin{pmatrix} -\cos(0) & -\sin(0) \\ -\sin(0) & \cos(0) \end{pmatrix} e^{-inbz} dz + \\ + \int_d^{2d} \begin{pmatrix} -\cos(2\pi/N) & -\sin(2\pi/N) \\ -\sin(2\pi/N) & \cos(2\pi/N) \end{pmatrix} e^{-inbz} dz + \dots + \int_{(N-1)d}^{Nd=a} \begin{pmatrix} -\cos\left(2\frac{\pi(N-1)}{N}\right) & -\sin\left(2\frac{\pi(N-1)}{N}\right) \\ -\sin\left(2\frac{\pi(N-1)}{N}\right) & \cos\left(2\frac{\pi(N-1)}{N}\right) \end{pmatrix} e^{-inbz} dz, \end{aligned} \quad (\text{S27})$$

where $d = a/N$ is a thickness of layers. If $n = 0$, each integral from equation (S27) reduces to d .

Therefore, taking into account (S25) and (S27) for $n = 0$, we obtain the following expression

$$\hat{\varepsilon}_0 = \bar{\varepsilon} \hat{I} + \Delta\varepsilon \frac{d}{a} \begin{pmatrix} M_{11} & M_{12} \\ M_{21} & M_{22} \end{pmatrix}. \quad (\text{S28})$$

Next we calculate the elements M_{11} , M_{12} , M_{21} and M_{22} from (S28) individually

$$M_{22} = -M_{11} = [1 + \cos(2\pi/N) + \cos(4\pi/N) + \dots + \cos(2(N-1)\pi/N)] = \sum_{n=0}^{N-1} \cos(2\pi n/N) = \delta_{1,N}, \quad (\text{S29})$$

$$M_{12} = M_{21} = -[0 + \sin(2\pi/N) + \sin(4\pi/N) + \dots + \sin(2(N-1)\pi/N)] = -\sum_{n=0}^{N-1} \sin(2\pi n/N) = 0. \quad (\text{S30})$$

The combination of (S28)-(S30) yields

$$\hat{\varepsilon}_0 = \bar{\varepsilon} \hat{I} + \Delta\varepsilon \begin{pmatrix} -1 & 0 \\ 0 & 1 \end{pmatrix} \delta_{1,N}. \quad (\text{S31})$$

Now consider the case when $n \neq 0$. Due to Eq. (S25), only the integral (S27) needs to be calculated. Examine a few integrals to establish the dependence

$$\int_0^d e^{-inbz} dz = e^{-i\pi nd/a} \frac{a}{\pi n} \sin\left(\frac{\pi nd}{a}\right), \quad (\text{S32})$$

$$\int_d^{2d} e^{-inbz} dz = e^{-3i\pi nd/a} \frac{a}{\pi n} \sin\left(\frac{\pi nd}{a}\right), \quad (\text{S33})$$

$$\int_{2d}^{3d} e^{-inbz} dz = e^{-5i\pi nd/a} \frac{a}{\pi n} \sin\left(\frac{\pi nd}{a}\right), \quad (\text{S34})$$

$$\int_{(N-1)d}^{Nd} e^{-inbz} dz = e^{-(2N-1)i\pi nd/a} \frac{a}{\pi n} \sin\left(\frac{\pi nd}{a}\right). \quad (\text{S35})$$

After substituting these values into equation (S27), we obtain a complex expression

$$\hat{\varepsilon}_n = \frac{\Delta\varepsilon}{\pi n} \sin\left(\frac{\pi nd}{a}\right) \begin{pmatrix} L_{11} & L_{12} \\ L_{21} & L_{22} \end{pmatrix}.$$

Similar to expressions (S29) and (S30), the elements L_{11} , L_{12} , L_{21} and L_{22} can be calculated separately

$$\begin{aligned} L_{22} = -L_{11} &= e^{-i\pi nd/a} + \cos\left(2\frac{\pi}{N}\right) e^{-3i\pi nd/a} + \cos\left(2\frac{2\pi}{N}\right) e^{-5i\pi nd/a} + \dots + \cos\left(2\frac{(N-1)\pi}{N}\right) e^{-(2n-1)i\pi nd/a} = \\ &= \sum_{m=0}^{N-1} \cos\left(2\frac{\pi m}{N}\right) e^{-i(2m+1)\pi n/N} = \sum_{m=0}^{N-1} \frac{1}{2} e^{-i\pi n/N} \left(e^{i[2m\pi(1-n)/N]} + e^{-i[2m\pi(1+n)/N]} \right) = \\ &= \frac{N}{2} e^{-i\pi n/N} \left(\sum_{k \in \mathbb{Z}} \delta_{1-Nk,n} + \sum_{k \in \mathbb{Z}} \delta_{Nk-1,n} \right), \end{aligned} \quad (\text{S36})$$

$$\begin{aligned} L_{12} = L_{21} &= -\left(\sin\left(2\frac{\pi}{N}\right) e^{-3i\pi nd/a} + \sin\left(2\frac{2\pi}{N}\right) e^{-5i\pi nd/a} + \dots + \sin\left(2\frac{(N-1)\pi}{N}\right) e^{-(2n-1)i\pi nd/a} \right) = \\ &= -\sum_{m=1}^{N-1} \sin\left(2\frac{\pi m}{N}\right) e^{-i(2m+1)\pi n/N} = i\frac{N}{2} e^{-i\pi n/N} \left(\sum_{k \in \mathbb{Z}} \delta_{1-Nk,n} - \sum_{k \in \mathbb{Z}} \delta_{Nk-1,n} \right). \end{aligned} \quad (\text{S37})$$

where k is an integer number.

Therefore, in general case the Fourier components for $n \neq 0$ can be presented as

$$\hat{\varepsilon}_n = \frac{N}{2} \frac{\Delta\varepsilon}{\pi n} \sin\left(\frac{\pi n}{N}\right) e^{-i\pi n/N} \left[\sum_{k \in \mathbb{Z}} \delta_{1-Nk, n} \begin{pmatrix} -1 & i \\ i & 1 \end{pmatrix} + \sum_{k \in \mathbb{Z}} \delta_{Nk-1, n} \begin{pmatrix} -1 & -i \\ -i & 1 \end{pmatrix} \right]. \quad (\text{S38})$$

If $N > 2$, then for every n no more than one term within two sums is nonzero. We can write

$$\hat{\varepsilon}_{1-Nk} = -(-1)^k \frac{N}{2} \frac{\Delta\varepsilon}{\pi(Nk-1)} \sin\left(\frac{\pi}{N}\right) \begin{pmatrix} -1 & i \\ i & 1 \end{pmatrix}, \quad \hat{\varepsilon}_{Nk-1} = (-1)^k \frac{N}{2} \frac{\Delta\varepsilon}{\pi(Nk-1)} \sin\left(\frac{\pi}{N}\right) \begin{pmatrix} -1 & -i \\ -i & 1 \end{pmatrix} \quad (\text{S39})$$

for any $k \in \mathbb{Z}$ and if n cannot be presented as $1 - Nk$ or $Nk - 1$, then the permittivity component $\hat{\varepsilon}_n$ vanishes.

B. Calculation of sums with commutative and anticommutative relations

The main text of the paper presents the results of computing the infinite sums, commutators and anticommutators involving Fourier components described by Eq. (S38). The commutation and anticommutation relations can be represented in the following form

$$[\hat{\varepsilon}_{Nk-1}, \hat{\varepsilon}_{1-Nk}] = -i \frac{N^2 \Delta\varepsilon^2}{\pi^2 (Nk-1)^2} \sin^2\left(\frac{\pi}{N}\right) \begin{pmatrix} 0 & -1 \\ 1 & 0 \end{pmatrix}, \quad (\text{S40})$$

$$[\hat{\varepsilon}_{1-Nk}, \hat{\varepsilon}_{Nk-1}] = i \frac{N^2 \Delta\varepsilon^2}{\pi^2 (Nk-1)^2} \sin^2\left(\frac{\pi}{N}\right) \begin{pmatrix} 0 & -1 \\ 1 & 0 \end{pmatrix}, \quad (\text{S41})$$

$$\{\hat{\varepsilon}_{Nk-1}, \hat{\varepsilon}_{1-Nk}\} = -\frac{N^2 \Delta\varepsilon^2}{\pi^2 (Nk-1)^2} \sin^2\left(\frac{\pi}{N}\right) \begin{pmatrix} 1 & 0 \\ 0 & 1 \end{pmatrix}, \quad (\text{S42})$$

$$\{\hat{\varepsilon}_{1-Nk}, \hat{\varepsilon}_{Nk-1}\} = -\frac{N^2 \Delta\varepsilon^2}{\pi^2 (Nk-1)^2} \sin^2\left(\frac{\pi}{N}\right) \begin{pmatrix} 1 & 0 \\ 0 & 1 \end{pmatrix} \quad (\text{S43})$$

and performed the sum with commutator

$$\begin{aligned} \sum_{n=1}^{\infty} \frac{[\hat{\varepsilon}_{-n}, \hat{\varepsilon}_n]}{n^3} &= \sum_{1-Nk>0}^{\infty} \frac{[\hat{\varepsilon}_{Nk-1}, \hat{\varepsilon}_{1-Nk}]}{(1-Nk)^3} + \sum_{Nk-1>0}^{\infty} \frac{[\hat{\varepsilon}_{1-Nk}, \hat{\varepsilon}_{Nk-1}]}{(Nk-1)^3} = \\ &= -i \frac{N^2 \Delta\varepsilon^2}{\pi^2} \sin^2\left(\frac{\pi}{N}\right) \begin{pmatrix} 0 & -1 \\ 1 & 0 \end{pmatrix} \left[\sum_{1-Nk>0}^{\infty} \frac{1}{(1-Nk)^5} - \sum_{Nk-1>0}^{\infty} \frac{1}{(Nk-1)^5} \right] \\ &= -i \frac{N^2 \Delta\varepsilon^2}{\pi^2} \sin^2\left(\frac{\pi}{N}\right) \begin{pmatrix} 0 & -1 \\ 1 & 0 \end{pmatrix} \left[\sum_{k=0}^{\infty} \frac{1}{(1+Nk)^5} - \sum_{k=1}^{\infty} \frac{1}{(Nk-1)^5} \right] = \end{aligned}$$

$$= -i \frac{\Delta \varepsilon^2 N^2}{\pi^2} \begin{pmatrix} 0 & -1 \\ 1 & 0 \end{pmatrix} \frac{\sin^2\left(\frac{\pi}{N}\right)}{24N^5} \left[\psi^{(4)}\left(\frac{1}{N}\right) - \psi^{(4)}\left(1 - \frac{1}{N}\right) \right] \quad (\text{S44})$$

and, analogously, the sum with anticommutator

$$\sum_{n=1}^{\infty} \frac{\{\hat{\varepsilon}_{-n}, \hat{\varepsilon}_n\}}{n^2} = \frac{\Delta \varepsilon^2 N^2}{\pi^2} \begin{pmatrix} 1 & 0 \\ 0 & 1 \end{pmatrix} \frac{\sin^2\left(\frac{\pi}{N}\right)}{6N^4} \left\{ \psi^{(3)}\left(\frac{1}{N}\right) + \psi^{(3)}\left(1 - \frac{1}{N}\right) \right\}, \quad (\text{S45})$$

where $\psi^{(m)}(z)$ is the polygamma function of order m , which is defined through the gamma function as follows

$$\psi^{(m)}(z) = \frac{d^{m+1}}{dz^{m+1}} \ln \Gamma(z).$$

As a result, the effective parameters for stepwise rotation of anisotropy axis can be written in the following form

$$\hat{\varepsilon}_{\text{eff}} = \hat{\text{I}} \bar{\varepsilon} + \Delta \varepsilon \begin{pmatrix} -1 & 0 \\ 0 & 1 \end{pmatrix} \delta_{1,N} + \hat{\text{I}} \frac{q^2}{b^2} \frac{\Delta \varepsilon^2}{\pi^2} \frac{\sin^2\left(\frac{\pi}{N}\right)}{6N^2} \left\{ \psi^{(3)}\left(\frac{1}{N}\right) + \psi^{(3)}\left(1 - \frac{1}{N}\right) \right\}, \quad (\text{S46})$$

$$\hat{\kappa}_{\text{eff}} = \hat{\text{I}} \frac{q^3}{b^3} \frac{\Delta \varepsilon^2}{\pi^2} \frac{\sin^2\left(\frac{\pi}{N}\right)}{24N^3} \left[\psi^{(4)}\left(\frac{1}{N}\right) - \psi^{(4)}\left(1 - \frac{1}{N}\right) \right]. \quad (\text{S47})$$

Analysing the limiting case ($N \rightarrow \infty$) in equations (S46) and (S47), we recover the material effective parameters for the medium with the continuous and uniform rotation of the anisotropy axis

$$\varepsilon'_{\text{eff}} = \bar{\varepsilon} + \Delta \varepsilon^2 \frac{q^2}{b^2}, \quad (\text{S48})$$

$$\kappa'_{\text{eff}} = -\Delta \varepsilon^2 \frac{q^3}{b^3}. \quad (\text{S49})$$

III. DERIVATION OF THE FULL CHIRALITY TENSOR

In this section, we derive full chirality tensor examining a general scenario with the arbitrary direction of the wave vector \mathbf{k} . Combining Floquet expansion with the wave equation, we recover

$$\begin{cases} -(k_z + nb)^2 E_{nx} + k_x(k_z + nb)E_{nz} + q^2 D_{nx} = 0, \\ k_x(k_z + nb)E_{nx} - k_x^2 E_{nz} + q^2 D_{nz} = 0, \\ -(k_z + nb)^2 E_{ny} - k_x^2 E_{ny} + q^2 D_{ny} = 0. \end{cases} \quad (\text{S50})$$

If the anisotropy axis rotates with coordinate as $\alpha(z) = \pi z/a$, then the Fourier components of permittivity tensor read

$$\hat{\varepsilon}_0 = \begin{pmatrix} \bar{\varepsilon} & 0 & 0 \\ 0 & \bar{\varepsilon} & 0 \\ 0 & 0 & \varepsilon_3 \end{pmatrix}, \quad \hat{\varepsilon}_1 = \frac{\Delta \varepsilon}{2} \begin{pmatrix} -1 & i & 0 \\ i & 1 & 0 \\ 0 & 0 & 0 \end{pmatrix}, \quad \hat{\varepsilon}_{-1} = \frac{\Delta \varepsilon}{2} \begin{pmatrix} -1 & -i & 0 \\ -i & 1 & 0 \\ 0 & 0 & 0 \end{pmatrix}. \quad (\text{S51})$$

At the same time, the Fourier components of inverse permittivity tensor take the form

$$\hat{\zeta}_0 = \frac{1}{\varepsilon_1 \varepsilon_2} \begin{pmatrix} \bar{\varepsilon} & 0 & 0 \\ 0 & \bar{\varepsilon} & 0 \\ 0 & 0 & \frac{\varepsilon_1 \varepsilon_2}{\varepsilon_3} \end{pmatrix}, \quad \hat{\zeta}_1 = \frac{\Delta \varepsilon}{2 \varepsilon_1 \varepsilon_2} \begin{pmatrix} 1 & -i & 0 \\ -i & -1 & 0 \\ 0 & 0 & 0 \end{pmatrix}, \quad \hat{\zeta}_{-1} = \frac{\Delta \varepsilon}{2 \varepsilon_1 \varepsilon_2} \begin{pmatrix} 1 & i & 0 \\ i & -1 & 0 \\ 0 & 0 & 0 \end{pmatrix}. \quad (\text{S52})$$

Introducing expansion parameter ξ explicitly, we recover the system of equations

$$\begin{cases} (\xi k_z + nb)^2 E_{nx} - \xi k_x (\xi k_z + nb) E_{nz} = \xi^2 q^2 D_{nx}, \\ E_{nz} = (\zeta_n)_{zi} D_{0i} + \sum_{m \neq 0} (\zeta_{n-m})_{zi} D_{mi}, \\ D_{nx} = (\varepsilon_n)_{xi} E_{0i} + \sum_{m \neq 0} (\varepsilon_{n-m})_{xi} E_{mi}, \\ \xi k_x D_{nx} + (\xi k_z + nb) D_{nz} = 0. \end{cases} \quad (\text{S53})$$

Expanding the Floquet harmonics of the fields in powers of small parameter, we obtain the following system of equations

$$\begin{cases} E_{ni} = E_{ni}^{(0)} + \xi E_{ni}^{(1)} + \xi^2 E_{ni}^{(2)} + \dots \\ D_{ni} = D_{ni}^{(0)} + \xi D_{ni}^{(1)} + \xi^2 D_{ni}^{(2)} + \dots \end{cases}. \quad (\text{S54})$$

From the first equation of system (S53) and system (S54) we obtain the following expression

$$\begin{aligned} (\xi^2 k_z^2 + 2\xi k_z nb + n^2 b^2)(E_{nx}^{(0)} + \xi E_{nx}^{(1)} + \xi^2 E_{nx}^{(2)} + \xi^3 E_{nx}^{(3)}) - (\xi^2 k_x k_z + \xi k_x nb) \cdot (E_{nz}^{(0)} + \xi E_{nz}^{(1)} + \xi^2 E_{nz}^{(2)} + \xi^3 E_{nz}^{(3)}) = \\ = \xi^2 q^2 (D_{nx}^{(0)} + \xi D_{nx}^{(1)} + \xi^2 D_{nx}^{(2)} + \xi^3 D_{nx}^{(3)}). \end{aligned} \quad (\text{S55})$$

Equating the terms with the same power of ξ results in the following expressions

$$E_{nx}^{(0)} = 0, \quad (\text{S56})$$

$$E_{nx}^{(1)} = \frac{k_x}{nb} E_{nz}^{(0)}, \quad (\text{S57})$$

$$E_{nx}^{(2)} = -\frac{k_x k_z}{n^2 b^2} E_{nz}^{(0)} + \frac{k_x}{nb} E_{nz}^{(1)} + \frac{q^2}{n^2 b^2} D_{nx}^{(0)}, \quad (\text{S58})$$

$$E_{nx}^{(3)} = \frac{q^2}{n^2 b^2} D_{nx}^{(1)} + \frac{k_x}{nb} E_{nz}^{(2)} + \frac{k_x k_z}{n^2 b^2} E_{nz}^{(1)} - \frac{2k_z}{nb} E_{nx}^{(2)} - \frac{k_z^2}{n^2 b^2} E_{nz}^{(1)}. \quad (\text{S59})$$

Analogous steps for electric displacement components lead to the following equation

$$(\xi k_z + nb)(D_{nz}^{(0)} + \xi D_{nz}^{(1)} + \xi^2 D_{nz}^{(2)} + \xi^3 D_{nz}^{(3)}) = -\xi k_x (D_{nx}^{(0)} + \xi D_{nx}^{(1)} + \xi^2 D_{nx}^{(2)} + \xi^3 D_{nx}^{(3)}), \quad (\text{S60})$$

which in turn yields

$$D_{nz}^{(0)} = 0, \quad (\text{S61})$$

$$D_{nz}^{(1)} = -\frac{k_x}{nb} D_{nx}^{(0)}, \quad (\text{S62})$$

$$D_{nz}^{(2)} = -\frac{k_x}{nb} D_{nx}^{(1)} + \frac{k_x k_z}{n^2 b^2} D_{nx}^{(0)}, \quad (\text{S63})$$

$$D_{nz}^{(3)} = -\frac{k_x}{nb} D_{nx}^{(2)} + \frac{k_x k_z}{n^2 b^2} D_{nx}^{(1)} - \frac{k_x k_z^2}{n^3 b^3} D_{nx}^{(0)}. \quad (\text{S64})$$

By combining the second and the third equations of the systems (S53) and (S54), we derive

$$E_{nz}^{(0)} = (\zeta_n)_{zi} D_{0i}, \quad (S65) \quad D_{nx}^{(0)} = (\varepsilon_n)_{xi} E_{0i}, \quad (S68)$$

$$E_{nz}^{(1)} = \sum_{m \neq 0} (\zeta_{n-m})_{zi} D_{mi}^{(1)}, \quad (S66) \quad D_{nx}^{(1)} = \sum_{m \neq 0} (\varepsilon_{n-m})_{xi} E_{mi}^{(1)}, \quad (S69)$$

$$E_{nz}^{(2)} = \sum_{m \neq 0} (\zeta_{n-m})_{zi} D_{mi}^{(2)}, \quad (S67) \quad D_{nx}^{(2)} = \sum_{m \neq 0} (\varepsilon_{n-m})_{xi} E_{mi}^{(2)}. \quad (S70)$$

For the zero Floquet harmonic ($n = 0$), which provides the major contribution, from the second and the third equations of system (S53) we have

$$\begin{cases} E_{0z} = (\zeta_0)_{zi} D_{0i} + \sum_{n \neq 0} (\zeta_{-n})_{zi} [D_{ni}^{(0)} + D_{ni}^{(1)} + D_{ni}^{(2)} + D_{ni}^{(3)}], \\ D_{0x} = (\varepsilon_0)_{xi} E_{0i} + \sum_{n \neq 0} (\varepsilon_{-n})_{xi} [E_{ni}^{(0)} + E_{ni}^{(1)} + E_{ni}^{(2)} + E_{ni}^{(3)}]. \end{cases} \quad (S71)$$

where we set the expansion parameter to 1 as in the original equations.

A. Zero and first order of perturbation theory

To find the zero and the first contributing terms in the system (S71), we analyze the following system of equations

$$\begin{cases} E_{0z} = (\zeta_0)_{zi} D_{0i} + \sum_{n \neq 0} (\zeta_{-n})_{zi} [D_{ni}^{(0)} + D_{ni}^{(1)}] \\ D_{0x} = (\varepsilon_0)_{xi} E_{0i} + \sum_{n \neq 0} (\varepsilon_{-n})_{xi} [E_{ni}^{(0)} + E_{ni}^{(1)}] \end{cases} \quad (S72)$$

For the first equation of the system (S72), the terms on the right-hand side with $n \neq 0$ vanish. This follows from the structure of the Fourier components of inverse permittivity (S52), where $(\zeta_1)_{zi} = (\zeta_{-1})_{zi} = 0$ for any i . It means that there is only one term left

$$D_{0z} = \varepsilon_3 E_{0z}. \quad (S73)$$

The second summand of the second equation of the system (S72) can be rewritten using (S56) in the following form

$$\begin{aligned} \sum_{n \neq 0} (\varepsilon_{-n})_{xi} [E_{ni}^{(0)} + E_{ni}^{(1)}] &= \sum_{n \neq 0} [(\varepsilon_{-n})_{xy} E_{ny}^{(0)} + (\varepsilon_{-n})_{xz} E_{nz}^{(0)} + \\ &+ (\varepsilon_{-n})_{xx} E_{nx}^{(1)} + (\varepsilon_{-n})_{xy} E_{ny}^{(1)} + (\varepsilon_{-n})_{xz} E_{nz}^{(1)}]. \end{aligned} \quad (S74)$$

According to (S51), $(\varepsilon_{-n})_{xz} = 0$ for any n . It means that the second and the last term of (S74) vanishes. Terms containing $E_{ny}^{(0)}$ and $E_{ny}^{(1)}$ are negligible too. Indeed, the third equation (S50) yields

$$E_{ny} = \frac{q^2}{k_x^2 + (k_z + nb)^2} D_{ny} = \frac{q^2}{n^2 b^2} \cdot \left(1 - \frac{k_z^2 + k_x^2 + 2k_z nb}{n^2 b^2}\right) D_{ny} + O(\xi^5). \quad (S75)$$

The analysis of the equation (S75) demonstrates that there is no contribution from $E_{ny}^{(0)}$ and $E_{ny}^{(1)}$. Therefore, the second equation of the system (S72) can be represented as

$$D_{0x} = (\varepsilon_0)_{xi} E_{0i} + \sum_{n \neq 0} ((\varepsilon_{-n})_{xx} E_{nx}^{(1)}). \quad (S76)$$

From equations (S57), (S62), (S65) and (S68) we obtain

$$\begin{cases} E_{nx}^{(1)} = \frac{k_x}{nb} (\zeta_n)_{zi} D_{0i}, \\ D_{nz}^{(1)} = -\frac{k_x}{nb} (\varepsilon_n)_{xi} E_{0i}. \end{cases} \quad (\text{S77})$$

By substituting the first equation of the (S77) into (S76), it immediately follows

$$\sum_{n \neq 0} (\varepsilon_{-n})_{xx} E_{nx}^{(1)} = \sum_{n \neq 0} (\varepsilon_{-n})_{xx} \frac{k_x}{nb} (\zeta_n)_{zi} D_{0i} = 0. \quad (\text{S78})$$

The last equality is valid since $(\zeta_1)_{zi} = (\zeta_{-1})_{zi} = 0$. Finally, the second equation of the system (S72) can be written in the following form

$$D_{0x} = \bar{\varepsilon} E_{0x}. \quad (\text{S79})$$

B. Second order of perturbation theory

The analysis of the second-order corrections to the fields reduces to the consideration of the following sums

$$\sum_{n \neq 0} (\varepsilon_{-n})_{xi} E_{ni}^{(2)} = \sum_{n \neq 0} \left[(\varepsilon_{-n})_{xx} E_{nx}^{(2)} + (\varepsilon_{-n})_{xy} E_{ny}^{(2)} \right], \quad (\text{S80})$$

$$\sum_{n \neq 0} (\zeta_{-n})_{zi} D_{ni}^{(2)} = \sum_{n \neq 0} \left[(\zeta_{-n})_{zx} D_{nx}^{(2)} + (\zeta_{-n})_{zy} D_{ny}^{(2)} \right]. \quad (\text{S81})$$

Consider the second order of E_{nx} . After substituting equations (S65), (S66) and (S68) into (S58), we obtain the following expression

$$\begin{aligned} & \sum_{n \neq 0} (\varepsilon_{-n})_{xx} E_{nx}^{(2)} = \\ & = - \sum_{n \neq 0} (\varepsilon_{-n})_{xx} \frac{k_x k_z}{n^2 b^2} (\zeta_n)_{zi} D_{0i} + \sum_{n \neq 0} (\varepsilon_{-n})_{xx} \frac{k_x}{nb} \sum_{m \neq 0} (\zeta_{n-m})_{zi} D_{mi}^{(1)} + \sum_{n \neq 0} (\varepsilon_{-n})_{xx} \frac{q^2}{n^2 b^2} (\varepsilon_n)_{xi} E_{0i}. \end{aligned} \quad (\text{S82})$$

The first term of equation (S82) equals to zero because of $(\zeta_{\pm 1})_{zi} = 0$:

$$- \sum_{n \neq 0} (\varepsilon_{-n})_{xx} \frac{k_x k_z}{n^2 b^2} (\zeta_n)_{zi} D_{0i} = 0.$$

There are only terms left on the second summand of (S82), when $n = m$: in this case $(\zeta_0)_{zz} \neq 0$. Taking into account the second expression of the system (S77), it is obtained

$$\begin{aligned} & \sum_{n \neq 0} (\varepsilon_{-n})_{xx} \frac{k_x}{nb} \sum_{m \neq 0} (\zeta_{n-m})_{zi} D_{mi}^{(1)} = - \sum_{n \neq 0} (\varepsilon_{-n})_{xx} \frac{k_x^2}{n^2 b^2} (\zeta_0)_{zz} (\varepsilon_n)_{xi} E_{0i} = \\ & = - \sum_{n \neq 0} (\varepsilon_{-n})_{xx} \frac{k_x^2}{n^2 b^2} \frac{1}{\varepsilon_3} \left((\varepsilon_n)_{xx} E_{0x} + (\varepsilon_n)_{xy} E_{0y} \right) = - \frac{1}{2\varepsilon_3} \left(\frac{k_x \Delta \varepsilon}{b} \right)^2 E_{0x}. \end{aligned} \quad (\text{S83})$$

The last term of the equation (S82) can be written explicitly as

$$\sum_{n \neq 0} (\varepsilon_{-n})_{xx} \frac{q^2}{n^2 b^2} (\varepsilon_n)_{xi} E_{0i} = \sum_{n \neq 0} (\varepsilon_n)_{xx} \frac{q^2}{n^2 b^2} \left((\varepsilon_n)_{xx} E_{0x} + (\varepsilon_n)_{xy} E_{0y} \right) = \frac{1}{2} \left(\frac{q \Delta \varepsilon}{b} \right)^2 E_{0x}. \quad (\text{S84})$$

Consider the second order of E_{ny} . By extracting the quadratic part on the small parameter from equation (S75), we obtain

$$E_{ny} = \frac{q^2}{n^2 b^2} D_{ny}. \quad (\text{S85})$$

Taking into account the connection between electric vector and electric displacement vector

$$D_{nk} = \sum_m (\varepsilon_{n-m})_{ki} E_{mi},$$

it is possible to write

$$D_{ny} = \sum_m (\varepsilon_{n-m})_{yi} E_{mi} = (\varepsilon_n)_{yi} E_{0i}. \quad (\text{S86})$$

After substituting (S86) to (S85), we have

$$E_{ny}^{(2)} = \frac{q^2}{n^2 b^2} (\varepsilon_n)_{yi} E_{0i} + O(\xi^3). \quad (\text{S87})$$

Finally, we can plug (S87) into (S80) and get

$$\sum_{n \neq 0} (\varepsilon_{-n})_{xy} \cdot \frac{q^2}{n^2 b^2} (\varepsilon_n)_{yi} E_{0i} = \sum_{n \neq 0} (\varepsilon_{-n})_{xy} \cdot \frac{q^2}{n^2 b^2} \left((\varepsilon_n)_{yx} E_{0x} + (\varepsilon_n)_{yy} E_{0y} \right) = \frac{1}{2} \left(\frac{q \Delta \varepsilon}{b} \right)^2 E_{0x}. \quad (\text{S88})$$

Therefore, equation (S80) can be written as

$$\sum_{n \neq 0} (\varepsilon_{-n})_{xi} E_{ni}^{(2)} = \frac{\Delta \varepsilon^2}{2b^2} \left(2q^2 - \frac{k_x^2}{\varepsilon_3} \right). \quad (\text{S89})$$

The sum (S81) vanishes due to $(\zeta_1)_{zi} = (\zeta_{-1})_{zi} = 0$.

Combining the components of the zero, the first and second order fields, we obtain

$$\begin{cases} D_{0z} = \varepsilon_3 E_{0z}, \\ D_{0x} = \left[\bar{\varepsilon} + \frac{\Delta \varepsilon^2}{2b^2} \left(2q^2 - \frac{k_x^2}{\varepsilon_3} \right) \right] E_{0x}. \end{cases} \quad (\text{S90})$$

To get effective parameters in the case of oblique incidence, it is necessary to know all components of the electric displacement vector. In order to find D_{0y} , we consider equation (S86):

$$D_{0y} = \sum_m (\varepsilon_{-m})_{yi} E_{mi} = \underbrace{(\varepsilon_0)_{yi} E_{0i}}_{\bar{\varepsilon} E_{0y}} + \sum_{n \neq 0} (\varepsilon_{-n})_{yi} E_{ni}^{(2)}. \quad (\text{S91})$$

Consider separately the second term of the equation (S91):

$$\sum_{n \neq 0} (\varepsilon_{-n})_{yi} E_{ni}^{(2)} = \sum_{n \neq 0} \left[(\varepsilon_{-n})_{yx} E_{nx}^{(2)} + (\varepsilon_{-n})_{yy} E_{ny}^{(2)} \right]. \quad (\text{S92})$$

Similar to expression (S82) for the $E_{nx}^{(2)}$ and using equation (S87), it can be obtained

$$\begin{aligned} \sum_{n \neq 0} (\varepsilon_{-n})_{yi} E_{ni}^{(2)} &= - \sum_{n \neq 0} (\varepsilon_{-n})_{yx} \frac{k_x k_z}{n^2 b^2} (\zeta_n)_{zi} D_{0i} + \sum_{n \neq 0} (\varepsilon_{-n})_{yx} \frac{k_x}{nb} \sum_{m \neq 0} (\zeta_{n-m})_{zi} D_{mi}^{(1)} + \\ &+ \sum_{n \neq 0} (\varepsilon_{-n})_{yx} \frac{q^2}{n^2 b^2} (\varepsilon_n)_{xi} E_{0i} + \sum_{n \neq 0} (\varepsilon_{-n})_{yy} \frac{q^2}{n^2 b^2} (\varepsilon_n)_{yi} E_{0i} = \frac{\Delta \varepsilon^2}{2b^2} \left(q^2 - \frac{k_x^2}{\varepsilon_3} \right) E_{0y} \end{aligned} \quad (\text{S93})$$

Therefore, the D_{0y} component with accuracy up to the second order of small parameter has the following form

$$D_{0y} = \left[\bar{\varepsilon} + \frac{\Delta\varepsilon^2}{2b^2} \left(2q^2 - \frac{k_x^2}{\varepsilon_3} \right) \right] E_{0y} \quad (\text{S94})$$

Merging (S95) and (S94) gives

$$\begin{cases} D_{0x} = \left[\bar{\varepsilon} + \frac{\Delta\varepsilon^2}{2b^2} \left(2q^2 - \frac{k_x^2}{\varepsilon_3} \right) \right] E_{0x}, \\ D_{0y} = \left[\bar{\varepsilon} + \frac{\Delta\varepsilon^2}{2b^2} \left(2q^2 - \frac{k_x^2}{\varepsilon_3} \right) \right] E_{0y}, \\ D_{0z} = \varepsilon_3 E_{0z}. \end{cases} \quad (\text{S95})$$

C. Third order of perturbation theory

However, to capture the effective chirality, one has to consider the third order of perturbation theory. We consider the following sum

$$\sum_{n \neq 0} (\varepsilon_{-n})_{xi} E_{ni}^{(3)} = \sum_{n \neq 0} (\varepsilon_{-n})_{xx} E_{nx}^{(3)} + \sum_{n \neq 0} (\varepsilon_{-n})_{xy} E_{ny}^{(3)} \quad (\text{S96})$$

To calculate the sum with $E_{nx}^{(3)}$, it is necessary to consider the equation (S59). First term in this equation vanishes:

$$\begin{aligned} D_{nx}^{(1)} &= \sum_{m \neq 0} \sum_{i=1}^3 (\varepsilon_{n-m})_{xi} E_{mi}^{(1)} = \sum_{m \neq 0} (\varepsilon_{n-m})_{xx} E_{mx}^{(1)} = \sum_{m \neq 0} (\varepsilon_{n-m})_{xx} \frac{k_x}{mb} E_{mz}^{(0)} = \\ &= \sum_{m \neq 0} (\varepsilon_{n-m})_{xx} \frac{k_x}{mb} (\zeta_m)_{zi} D_{0i} = 0, \end{aligned} \quad (\text{S97})$$

where it was taken into account that $E_{my}^{(1)} = 0$ and $\zeta_{\pm 1} = 0$. The term with $E_{mz}^{(1)}$ also vanishes due to $(\varepsilon_{n-m})_{xz} = 0$.

The second term in equation (S59) when substituted into equation (S96) reduces to

$$\sum_{n \neq 0} (\varepsilon_{-n})_{xx} \frac{k_x}{nb} \sum_{m \neq 0} (\zeta_{n-m})_{zi} D_{mi}^{(2)}, \quad (\text{S98})$$

where equation (S67) was used.

It is obtained non-zero value if $n = m$ and $i = z$:

$$\sum_{n \neq 0} (\varepsilon_{-n})_{xx} \frac{k_x}{nb} (\zeta_0)_{zz} D_{nz}^{(2)}. \quad (\text{S99})$$

Using equation (S63) we get 2 sums. We examine the first one:

$$\begin{aligned} - \sum_{n \neq 0} (\varepsilon_{-n})_{xx} \frac{k_x^2}{n^2 b^2} \frac{1}{\varepsilon_3} D_{nx}^{(1)} &= - \frac{1}{\varepsilon_3} \sum_{n \neq 0} (\varepsilon_{-n})_{xx} \frac{k_x^2}{n^2 b^2} \sum_{m \neq 0} \left[(\varepsilon_{n-m})_{xx} E_{mx}^{(1)} + (\varepsilon_{n-m})_{xy} E_{my}^{(1)} \right] = \\ &= - \frac{1}{\varepsilon_3} \sum_{n \neq 0} (\varepsilon_{-n})_{xx} \frac{k_x^2}{n^2 b^2} \sum_{m \neq 0} (\varepsilon_{n-m})_{xx} \frac{k_x}{mb} (\zeta_m)_{zi} D_{0i} = 0, \end{aligned} \quad (\text{S100})$$

where the last equality is valid due to $(\zeta_{\pm 1})_{zi} = 0$ for any i .

The second one sum reduces to

$$\begin{aligned} \sum_{n \neq 0} (\varepsilon_{-n})_{xx} \frac{k_x^2 k_z}{n^3 b^3} \frac{1}{\varepsilon_3} (\varepsilon_n)_{xi} E_{0i} &= \sum_{n \neq 0} (\varepsilon_{-n})_{xx} \frac{k_x^2 k_z}{n^3 b^3} \frac{1}{\varepsilon_3} [(\varepsilon_n)_{xx} E_{0x} + (\varepsilon_n)_{xy} E_{0y}] = \\ &= -i \frac{\Delta \varepsilon^2}{2} \frac{k_x^2 k_z}{\varepsilon_3 b^3} E_{0y}. \end{aligned} \quad (\text{S101})$$

The third term in equation (S59) when substituted into equation (S96) reduces to

$$\begin{aligned} \sum_{n \neq 0} (\varepsilon_{-n})_{xx} \frac{k_x k_z}{n^2 b^2} \sum_{m \neq 0} (\zeta_{n-m})_{zi} D_{mi}^{(1)} &= \sum_{n \neq 0} (\varepsilon_{-n})_{xx} \frac{k_x^2 k_z}{n^3 b^3} \frac{1}{\varepsilon_3} (\varepsilon_n)_{xi} E_{0i} = \\ &= i \frac{\Delta \varepsilon^2}{2} \frac{k_x^2 k_z}{\varepsilon_3 b^3} E_{0y}. \end{aligned} \quad (\text{S102})$$

The fourth term in equation (S59) when substituted into equation (S96) reduces to

$$- \sum_{n \neq 0} (\varepsilon_{-n})_{xx} \frac{2k_z}{nb} E_{nx}^{(2)}. \quad (\text{S103})$$

Here we need to substitute the equation (S58) and take into account expressions (S66) and (S68) as follows

$$E_{nx}^{(2)} = - \frac{k_x k_z}{n^2 b^2} (\zeta_n)_{zi} D_{0i} + \frac{k_x}{nb} \sum_{m \neq 0} (\zeta_{n-m})_{zi} D_{mi}^{(1)} + \frac{q^2}{n^2 b^2} (\varepsilon_n)_{xi} E_{0i}. \quad (\text{S104})$$

After substituting the expression (S104) into equation (S103), the first term will vanish. The second term can be written as

$$\begin{aligned} - \sum_{n \neq 0} (\varepsilon_{-n})_{xx} \frac{2k_z k_x}{n^2 b^2} \sum_{m \neq 0} (\zeta_{n-m})_{zi} D_{mi}^{(1)} &= \sum_{n \neq 0} (\varepsilon_{-n})_{xx} \frac{2k_z k_x^2}{n^3 b^3} \frac{1}{\varepsilon_3} [(\varepsilon_n)_{xx} E_{0x} + (\varepsilon_n)_{xy} E_{0y}] = \\ &= -i \Delta \varepsilon^2 \frac{k_x^2 k_z}{\varepsilon_3 b^3} E_{0y}. \end{aligned} \quad (\text{S105})$$

The third term reduces to

$$- \sum_{n \neq 0} (\varepsilon_{-n})_{xx} \frac{2k_z q^2}{n^3 b^3} (\varepsilon_n)_{xi} E_{0i} = i \Delta \varepsilon^2 \frac{k_z q^2}{b^3} E_{0y}. \quad (\text{S106})$$

The fifth term in equation (S59) when substituted into equation (S96) reduces to zero due to $(\zeta_{\pm 1})_{zi} = 0$ for any i . Therefore, the first part for the equation (S96) can be written as

$$\sum_{n \neq 0} (\varepsilon_{-n})_{xx} E_{nx}^{(3)} = i \Delta \varepsilon^2 \frac{k_z}{b^3} \left(q^2 - \frac{k_x^2}{\varepsilon_3} \right) \quad (\text{S107})$$

To get the second part, consisting $E_{ny}^{(3)}$, it is necessary to return to the equation (S75) and select the component proportional to ξ^3 . Substituting there the expression (S86), we obtain the following equation

$$E_{ny}^{(3)} = - \frac{2k_z q^2}{n^3 b^3} \sum_{i=1}^3 (\varepsilon_n)_{yi} E_{0i}. \quad (\text{S108})$$

Substituting it into sum leads us to the following expression

$$\sum_{n \neq 0} (\varepsilon_{-n})_{xy} E_{ny}^{(3)} = i \Delta \varepsilon^2 \frac{k_z q^2}{b^3} E_{0y} \quad (\text{S109})$$

Therefore, D_{0x} with accuracy up to the third order of small parameter has the following form

$$D_{0x} = \left[\bar{\varepsilon} + \frac{\Delta \varepsilon^2}{2b^2} \left(2q^2 + \frac{k_x^2}{\varepsilon_3} \right) \right] E_{0x} + i \frac{\Delta \varepsilon^2 k_z}{b^3} \left(2q^2 - \frac{k_x^2}{\varepsilon_3} \right) E_{0y}. \quad (\text{S110})$$

In a similar way, D_{0y} can be found as

$$D_{0y} = (\varepsilon_0)_{yi} E_{oi} + \sum_{n \neq 0} (\varepsilon_{-n})_{yi} E_{ni}^{(3)}. \quad (\text{S111})$$

The first summation is reduced to $\bar{\varepsilon} E_{0y}$. In the second summation it is necessary to do the same calculations but replace $(\varepsilon_{-n})_{xi}$ on $(\varepsilon_{-n})_{yi}$. Therefore, the equation for D_{0y} with accuracy up to the third order of small parameter has the following form

$$D_{0y} = \left[\bar{\varepsilon} + \frac{\Delta \varepsilon^2}{2b^2} \left(2q^2 - \frac{k_x^2}{\varepsilon_3} \right) \right] E_{0y} - i \frac{\Delta \varepsilon^2 k_z}{b^3} \left(2q^2 - \frac{k_x^2}{\varepsilon_3} \right) E_{0x}. \quad (\text{S112})$$

Finally, the connection between electric displacement vector and the electric field with accuracy up to the third order of a small parameter a/λ for the structure consisting of anisotropic infinitely thin layers with continuously rotating anisotropy axis has the form

$$\begin{cases} D_{0x} = \left[\bar{\varepsilon} + \frac{\Delta \varepsilon^2}{2b^2} \left(2q^2 - \frac{k_x^2}{\varepsilon_3} \right) \right] E_{0x} + i \frac{\Delta \varepsilon^2 k_z}{b^3} \left(2q^2 - \frac{k_x^2}{\varepsilon_3} \right) E_{0y}, \\ D_{0y} = \left[\bar{\varepsilon} + \frac{\Delta \varepsilon^2}{2b^2} \left(2q^2 - \frac{k_x^2}{\varepsilon_3} \right) \right] E_{0y} - i \frac{\Delta \varepsilon^2 k_z}{b^3} \left(2q^2 - \frac{k_x^2}{\varepsilon_3} \right) E_{0x}, \\ D_{0z} = \varepsilon_3 E_{0z}. \end{cases} \quad (\text{S113})$$

D. Reducing the material equations to canonical bianisotropic form

Equations (S113) provide the constitutive relations for the averaged fields in the nonlocal (spatially dispersive) framework. To convert these to the more convenient bianisotropic form, we redefine the auxiliary fields \mathbf{H} and \mathbf{D} such that Maxwell's equations are kept invariant.

To that end, we denote some factors in the (S113) for simplicity as follows

$$A = \bar{\varepsilon} + \frac{\Delta \varepsilon^2}{2b^2} \left(2q^2 - \frac{k_x^2}{\varepsilon_3} \right), \quad (\text{S114})$$

$$B = \frac{\Delta \varepsilon^2}{b^3} \left(2q^2 - \frac{k_x^2}{\varepsilon_3} \right). \quad (\text{S115})$$

Hence, the system of equations (S113) can be rewritten as follows

$$\begin{cases} D_{0x} = AE_{0x} + ik_z B E_{0y}, \\ D_{0y} = -ik_z B E_{0x} + AE_{0y}, \\ D_{0z} = \varepsilon_3 E_{0z} \end{cases} \quad (\text{S116})$$

or

$$\mathbf{D}_0 = \hat{\varepsilon}_{\text{eff}} \mathbf{E}_0 - i B k_z \hat{e}_z^\times \mathbf{E}_0 \quad (\text{S117})$$

where

$$\hat{\varepsilon}_{\text{eff}} = \begin{pmatrix} A & 0 & 0 \\ 0 & A & 0 \\ 0 & 0 & \varepsilon_3 \end{pmatrix} \quad \text{and} \quad \hat{e}_z^\times = \begin{pmatrix} 0 & -1 & 0 \\ 1 & 0 & 0 \\ 0 & 0 & 0 \end{pmatrix}. \quad (\text{S118})$$

Similar to normal incidence case, to reduce the material equations to canonical bianisotropic form, it is necessary to redefine magnetic field \mathbf{H}_0 as follows

$$\mathbf{H}_0 = \mathbf{B}_0 - i\hat{\kappa}\mathbf{E}_0. \quad (\text{S119})$$

Consider the following Maxwell's equation for the monochromatic plane wave

$$\mathbf{k} \times \mathbf{H}_0 = -q\mathbf{D}'_0. \quad (\text{S120})$$

Expressing \mathbf{D}'_0 from the equation (S120) and substituting there vector \mathbf{H}_0 lead us to the following redefinition of electric displacement:

$$\mathbf{D}'_0 = \mathbf{D}_0 + \frac{i}{q}\hat{k}^\times \hat{\kappa}\mathbf{E}_0, \quad (\text{S121})$$

where

$$\hat{k}^\times = \begin{pmatrix} 0 & -k_z & 0 \\ k_z & 0 & -k_x \\ 0 & k_x & 0 \end{pmatrix}. \quad (\text{S122})$$

After substituting (S117) to (S121), we obtain

$$\mathbf{D}'_0 = \hat{\varepsilon}_{\text{eff}}\mathbf{E}_0 - iBk_z\hat{e}_z^\times\mathbf{E}_0 + \frac{i}{q}\hat{k}^\times\hat{\kappa}\mathbf{E}_0. \quad (\text{S123})$$

On the other hand, to obtain the conventional material equations with chirality tensor, the following equation should be fulfilled:

$$-iBk_z\hat{e}_z^\times\mathbf{E}_0 + \frac{i}{q}\hat{k}^\times\hat{\kappa}\mathbf{E}_0 = i\hat{\kappa}\mathbf{H}_0. \quad (\text{S124})$$

From equations (S119) and (S124) it follows

$$-Bk_z\hat{e}_z^\times\mathbf{E}_0 + \frac{1}{q}\hat{k}^\times\hat{\kappa}\mathbf{E}_0 = \hat{\kappa}\mathbf{B}_0 \quad (\text{S125})$$

or by applying Maxwell's equation for monochromatic plane wave

$$\hat{k}^\times\hat{\kappa} - \hat{\kappa}\hat{k}^\times = qBk_z\hat{e}_z^\times \quad (\text{S126})$$

where the $\hat{\kappa}^2$ term is neglected due to its smallness.

This is the matrix equation on $\hat{\kappa}$. The solution of matrix equation (S126) has the following form

$$\hat{\kappa}_{\text{eff}} = -\frac{1}{2} \begin{pmatrix} qB & 0 & 0 \\ 0 & qB & 0 \\ 0 & 0 & -qB \end{pmatrix}. \quad (\text{S127})$$

Hence, the effective parameters comprising bianisotropic constitutive relations for the general direction of the wave vector have the following form

$$\hat{\varepsilon}_{\text{eff}} = \begin{pmatrix} \bar{\varepsilon} + \frac{\Delta\varepsilon^2}{2b^2} \left(2q^2 - \frac{k_x^2}{\varepsilon_3} \right) & 0 & 0 \\ 0 & \bar{\varepsilon} + \frac{\Delta\varepsilon^2}{2b^2} \left(2q^2 - \frac{k_x^2}{\varepsilon_3} \right) & 0 \\ 0 & 0 & \varepsilon_3 \end{pmatrix}, \quad (\text{S128})$$

$$\hat{\kappa}_{\text{eff}} = -\frac{q}{2} \frac{\Delta\varepsilon^2}{b^3} \left(2q^2 - \frac{k_x^2}{\varepsilon_3} \right) \begin{pmatrix} 1 & 0 & 0 \\ 0 & 1 & 0 \\ 0 & 0 & -1 \end{pmatrix}. \quad (\text{S129})$$

-
- [1] S. Y. Vetrov, I. V. Timofeev, and V. F. Shabanov, Localized modes in chiral photonic structures, *Physics-Uspekhi* **63**, 33 (2020).
- [2] K. V. Voronin, A. N. Toksumakov, G. A. Ermolaev, A. S. Slavich, M. K. Tatmyshevskiy, S. M. Novikov, A. A. Vyshnevyy, A. V. Arsenin, K. S. Novoselov, D. A. Ghazaryan, *et al.*, Chiral Photonic Super-Crystals Based on Helical van der Waals Homostructures, *Laser & Photonics Reviews* **18**, 2301113 (2024).